

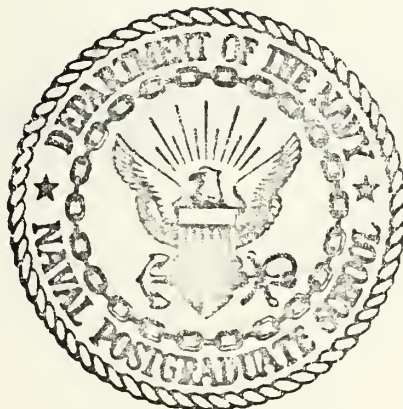
MONTHLY HEAT BUDGET CALCULATIONS  
FROM THE EASTERN NORTH PACIFIC OCEAN  
USING SYNOPTIC-SCALE DATA

Robert Timothy Schnoor

DURUM, MAX LIBRARY  
NAVAL POSTGRADUATE SCHOOL  
MONTEREY, CALIFORNIA 93940

# NAVAL POSTGRADUATE SCHOOL

## Monterey, California



# THESIS

MONTHLY HEAT BUDGET CALCULATIONS  
FOR THE EASTERN NORTH PACIFIC OCEAN  
USING SYNOPTIC-SCALE DATA

by

Robert Timothy Schnoor

June 1975

Thesis Advisor:

R.L. Elsberry

Approved for public release; distribution unlimited.

Prepared for: Naval Oceanographic Office  
Washington, D.C. 20373

T167969



NAVAL POSTGRADUATE SCHOOL  
Monterey, California

Rear Admiral Isham Linder  
Superintendent

Jack R. Borsting  
Provost

This thesis prepared in conjunction with research support in part by  
Naval Oceanographic Office, Code 5220, under Job Order Number 611G-0042.

Reproduction of all or part of this report is authorized.



REPORT DOCUMENTATION PAGE		READ INSTRUCTIONS BEFORE COMPLETING FORM
1. REPORT NUMBER NPS-51Es75061	2. GOVT ACCESSION NO.	3. RECIPIENT'S CATALOG NUMBER
4. TITLE (and Subtitle) Monthly Heat Budget Calculations for the Eastern North Pacific Ocean Using Synoptic-Scale Data		5. TYPE OF REPORT & PERIOD COVERED Thesis September 1974-June 1975
		6. PERFORMING ORG. REPORT NUMBER
7. AUTHOR(s) Robert Timothy Schnoor in conjunction with Russell L. Elsberry		8. CONTRACT OR GRANT NUMBER(s)
9. PERFORMING ORGANIZATION NAME AND ADDRESS Naval Postgraduate School Monterey, California 93940		10. PROGRAM ELEMENT, PROJECT, TASK AREA & WORK UNIT NUMBERS N62306-75-WR-5-0046
11. CONTROLLING OFFICE NAME AND ADDRESS Naval Oceanographic Office, Code 5220 Washington, D.C. 20373		12. REPORT DATE June 1975
		13. NUMBER OF PAGES
14. MONITORING AGENCY NAME & ADDRESS (if different from Controlling Office)		15. SECURITY CLASS. (of this report)  Unclassified
		15a. DECLASSIFICATION/DOWNGRADING SCHEDULE
16. DISTRIBUTION STATEMENT (of this Report)  Approved for public release; distribution unlimited		
17. DISTRIBUTION STATEMENT (of the abstract entered in Block 20, if different from Report)		
18. SUPPLEMENTARY NOTES		
19. KEY WORDS (Continue on reverse side if necessary and identify by block number) Oceanic heat budget Air-Sea interaction Eastern North Pacific Ocean Oceanic heat storage		
20. ABSTRACT (Continue on reverse side if necessary and identify by block number) A heat budget was calculated for the upper 250 m of the eastern North Pacific Ocean using data from Fleet Numerical Weather Central. The motivation for the study is the proposed ocean basin application of mixed-layer models. The heat budget calculation indirectly determined the magnitude of subsurface physical processes by comparing the monthly change in heat storage with the net air-sea heat flux. The heat storage values were derived from subsurface thermal structure data and compared to two different computations of heat flux data. In certain areas physical processes, as found by Bathen		







Block 20:

(1971), are two to three times greater than the heat flux. However, in the mean the values are of the same magnitude as the heat flux. Investigation of the heat storage term of the heat budget equation indicates that larger values of the residual term may be due to computational error. Present mixed-layer models which rely solely on the heat flux to balance heat storage changes must be modified to include physical processes for application to ocean basins.



Monthly Heat Budget Calculations  
for the Eastern North Pacific Ocean  
Using Synoptic-Scale Data

by

Robert Timothy Schnoor  
Ensign, United States Navy  
B.S., United States Naval Academy, 1974

Submitted in partial fulfillment of the  
requirements for the degree of

MASTER OF SCIENCE IN METEOROLOGY

from the  
NAVAL POSTGRADUATE SCHOOL

June 1975



## ABSTRACT

A heat budget was calculated for the upper 250 m of the eastern North Pacific Ocean using data from Fleet Numerical Weather Central. The motivation for the study is the proposed ocean basin application of mixed-layer models. The heat budget calculation indirectly determined the magnitude of subsurface physical processes by comparing the monthly change in heat storage with the net air-sea heat flux. The heat storage values were derived from subsurface thermal structure data and compared to two different computations of heat flux data. In certain areas physical processes, as found by Bathen (1971), are two to three times greater than the heat flux. However, in the mean the values are of the same magnitude as the heat flux. Investigation of the heat storage term of the heat budget equation indicates that larger values of the residual term may be due to computational error. Present mixed-layer models which rely solely on the heat flux to balance heat storage changes must be modified to include physical processes for application to ocean basins.



# TABLE OF CONTENTS

I.	INTRODUCTION AND BACKGROUND . . . . .	9
II.	THE HEAT BUDGET EQUATION . . . . .	12
III.	SOURCES AND USAGE OF DATA . . . . .	15
IV.	DISCUSSION OF RESULTS . . . . .	17
	A. EXAMPLES OF THE HEAT BUDGET CALCULATION . . . . .	17
	B. AIR-SEA HEAT FLUX TERM . . . . .	25
	C. THE HEAT STORAGE TERM . . . . .	37
V.	SUMMARY AND CONCLUSIONS . . . . .	50
	APPENDIX A FNWC COMPUTERIZED PRODUCTS . . . . .	54
	APPENDIX B FNWC OBJECTIVE ANALYSIS . . . . .	55
	APPENDIX C NMFS COMPUTATIONAL PROCEDURES . . . . .	56
	BIBLIOGRAPHY . . . . .	65
	INITIAL DISTRIBUTION LIST . . . . .	66

See also Elliott, Dec 1973, Thesis  
E-3685





## LIST OF FIGURES

### Figure

1. Notations Used in the Heat Budget Equation . . . . .	13
2. Heat Storage Change--15 June to 15 July 1974 . . . . .	20
3. Total Heat Exchange ( $Q_n$ ) Analysis--15 June to 15 July 1974 . . . . .	22
4. Computed Residual Using $Q_n$ values of Heat Flux 15 June to 15 July 1974 . . . . .	23
5. Heat Storage Change--15 November to 15 December 1974 . . . . .	24
6. Total Heat Exchange ( $Q_n$ ) Analysis--15 November to 15 December 1974 . . . . .	26
7. Computed Residual Using $Q_n$ Values of Heat Flux 15 November to 15 December 1974 . . . . .	27
8. Comparison of Heat Flux Values at OWS November . . . . .	29
9. 1961-1971 Mean Net Heat Flux Derived by Clark et al. (1974) for 15 June to 15 July . . . . .	30
10. Total Heat Flux (THF) Analysis--15 June to 15 July 1974 . . . . .	31
11. 1961-1971 Mean Net Heat Flux Derived by Clark et al. (1974) for 15 November to 15 December . . . . .	32
12. Total Heat Flux (THF) Analysis--15 November to 15 December 1974 . . . . .	33
13. Computed Residual Using THF Values of Heat Flux-- 15 June to 15 July 1974 . . . . .	35
14. Computed Residual Using THF Values of Heat Flux-- 15 November to 15 December 1974 . . . . .	36
15. 1974 Monthly Mean and Long-Term Mean Temperature Profiles for June and July near OWS November . . . . .	38
16. 1974 Monthly Mean and Long-Term Mean Temperature Profiles for July and August near OWS November . . . . .	39



17.	1974 Monthly Mean and Long-Term Mean Temperature Profiles for June and July near 15N,140W . . . . .	40
18.	1974 Monthly Mean and Long-Term Mean Temperature Profiles for July and August near 15N,140W . . . . .	41
19.	Great Circle Route Between Hawaii and San Francisco and Gridpoints of FNWC Data Used in the Heat Storage Comparison . . . . .	45
20.	Comparison of NMFS Mean Heat Storage Values for June 1974 with FNWC Monthly and Long-Term Means . . . . .	46
21.	Comparison of NMFS Mean Heat Storage Values for November 1974 with FNWC Monthly and Long-Term Means . . . . .	47
22.	Time Cross-Section of NMFS Heat Storage Values . . . . .	48
23.	Percentage of FNWC Grid Covered by Significant Values of the Computed Residual . . . . .	52



#### ACKNOWLEDGEMENTS

The author wishes to express his sincerest appreciation to Dr. R. L. Elsberry, Department of Meteorology, Naval Postgraduate School, for his time, interest, and guidance during this study; and to Dr. R. L. Haney for his comments and review of the thesis.

Appreciation is also due to the Fleet Numerical Weather Central Climatology Department for providing the data and computer time; and to Dr. D. R. McLain, National Marine Fisheries Service, for his assistance in providing an invaluable second source of data.





## I. INTRODUCTION AND BACKGROUND

The effectiveness of Naval Anti-Submarine Warfare operations is highly dependent upon an accurate prediction of sonar ranges. Recent development of various acoustical forecasting models has emphasized the need for accurate predictions of the ocean thermal structure. Variations in the vertical sound velocity profile are determined by changes in the ocean thermal structure, which occur mainly in the well-mixed surface layer and the thermocline.

The exchange of heat and momentum at the air-sea interface and the processes of advection, diffusion and mixing below the sea surface are the factors which affect changes in the ocean thermal structure. Momentum transfer to the ocean and the resulting generation and breaking of waves leads to turbulence which affects the depth of the mixed layer. When the net heat flux results in surface cooling, convective overturning is generated with subsequent deepening of the mixed layer, while net heating leads to shallower surface layers. Advection, diffusion and mixing processes produce changes in the ocean thermal structure by the horizontal and vertical movement of water below the sea surface.

It is difficult to accurately represent all of these processes in an ocean thermal structure prediction model for three reasons. First, each process is a complex result of numerous other interactions occurring in the ocean and atmosphere. Second, the time and space scales affect the relative importance of each process. Finally, the data required for parameterization of the processes and initialization of prediction models have either been continuously measured at only a few selected locations in the ocean, or are not directly measurable by presently available means.



Numerous models of the oceanic mixed layer, based on the early theory of Kraus and Turner (1967), have been developed. The basic hypothesis of mixed-layer models is that deviations from the climatological sea-surface temperature fields can be directly attributed to local atmospheric inputs without involving the deep ocean. In general these models do not consider horizontal advection, since they are local treatments and tested with point measurements. Gill and Niiler (1973) showed that for time scales on the order of a season, heat input is mainly stored locally, and the larger the region the smaller the effect of horizontal advection. On smaller space and time scales, Bowden, Howe and Tait (1970) found from nearly continuous bathythermograph soundings that the diurnal changes in the heat budget evolved in a pattern grossly similar to seasonal changes which have been simulated with mixed-layer models. The larger variations in heat storage compared to variations in heat input were attributed to advection.

Essentially mixed-layer models are just heat storage calculations in the layer above the seasonal thermocline, the depth of which is predicted by the theory. Heat budget studies have been performed on various time and space scales to determine the relative importance of each process affecting the ocean thermal structure. Seckel (1962) formulated a simple heat budget in which the rate of change of heat storage in the mixed layer was balanced by the net air-sea heat flux and the heat transported in and out by currents. Seckel assumed that horizontal and vertical diffusion were relatively small compared to the other processes. Seckel noted the high stability of the thermocline in the Hawaiian island region and limited his budget to the well-mixed surface layer. He constructed advection diagrams for monthly time periods in three degree squares around Hawaii.



Wyrтки and Haberland (1968) analyzed separately the processes that maintain the heat distribution and storage in the North Pacific Ocean. They determined that horizontal diffusion can contribute significantly to heat transports in areas of strong temperature gradients, and that advection must be the most important factor in determining the temperature distribution in strong boundary currents. However, they stated that variations in the mixed layer depth are of greater importance in regions of zonal flow.

Bathen (1971) assumed that the vertical processes of heat advection and mixing balanced each other in the upper 250 meters of the ocean. He found that the processes of surface heat flux, horizontal advection and horizontal diffusion with annual averages of 29%, 63% and 8%, respectively, contributed to the local monthly change in the heat storage for the North Pacific Ocean basin.

The purpose of this study is to calculate a similar heat budget to determine the relative importance of the processes that influence the ocean thermal structure. If, as determined by Gill and Niiler (1973), the monthly change in heat storage is balanced by the local air-sea heat flux, then the application of present mixed-layer models can be readily expanded to ocean basin regions for these shorter time scales. On the other hand, if the processes of advection, diffusion, and mixing are equal to, or greater in importance than the heat flux, as shown by Bathen (1971), then mixed-layer models must be modified to include these additional processes. The procedure used here treated the processes of advection and diffusion as a single process and compared it to the net heat flux, using readily available data from Fleet Numerical Weather Central (FNWC).



## II. THE HEAT BUDGET EQUATION

The equation governing the processes involved in the redistribution of heat in the ocean are written following Wyrтки and Haberland (1968). Using integral relationships the equation is that of conservation of heat in a given volume:

$$\begin{aligned} \int_0^D \int_1 (H \vec{v} - A^h \nabla H) \cdot \vec{n} \, dz \, dl + \iint_{\text{Bottom of cylinder}} (wH - A \frac{\partial H}{\partial z})_D \, dx \, dy \\ + \iint_{\text{surface}} Q \, dx \, dy = \frac{\partial}{\partial t} \iiint_{\text{volume}} H \, dz \, dx \, dy \end{aligned} \quad (1)$$

where:  $\vec{v}$  = horizontal velocity vector  
 $H$  = total heat storage in cal cm<sup>-2</sup>  
 $\vec{n}$  = unit vector perpendicular to the vertical walls of the enclosed volume, directed inward  
 $w$  = vertical velocity at the bottom of the cylinder  
 $A^h$  = horizontal eddy diffusion coefficient  
 $A$  = vertical eddy diffusion coefficient  
 $D$  = depth of the cylinder as illustrated in Figure 1  
 $Q$  = net downward heat flux at the surface cal cm<sup>-2</sup> day<sup>-1</sup>  
 $\nabla$  = the two dimensional del operator

The first integral in equation (1) describes the flow of heat through the walls of the cylinder by horizontal advection and diffusion; the second term, the vertical advection and diffusion; the third term, the net heat flux; and the right hand side of the equation, the time change of heat storage of the volume. Dividing by the surface area of the cylinder, integrating over the depth of the water column, and taking the limit of an infinitely small surface area, equation (1) is written:





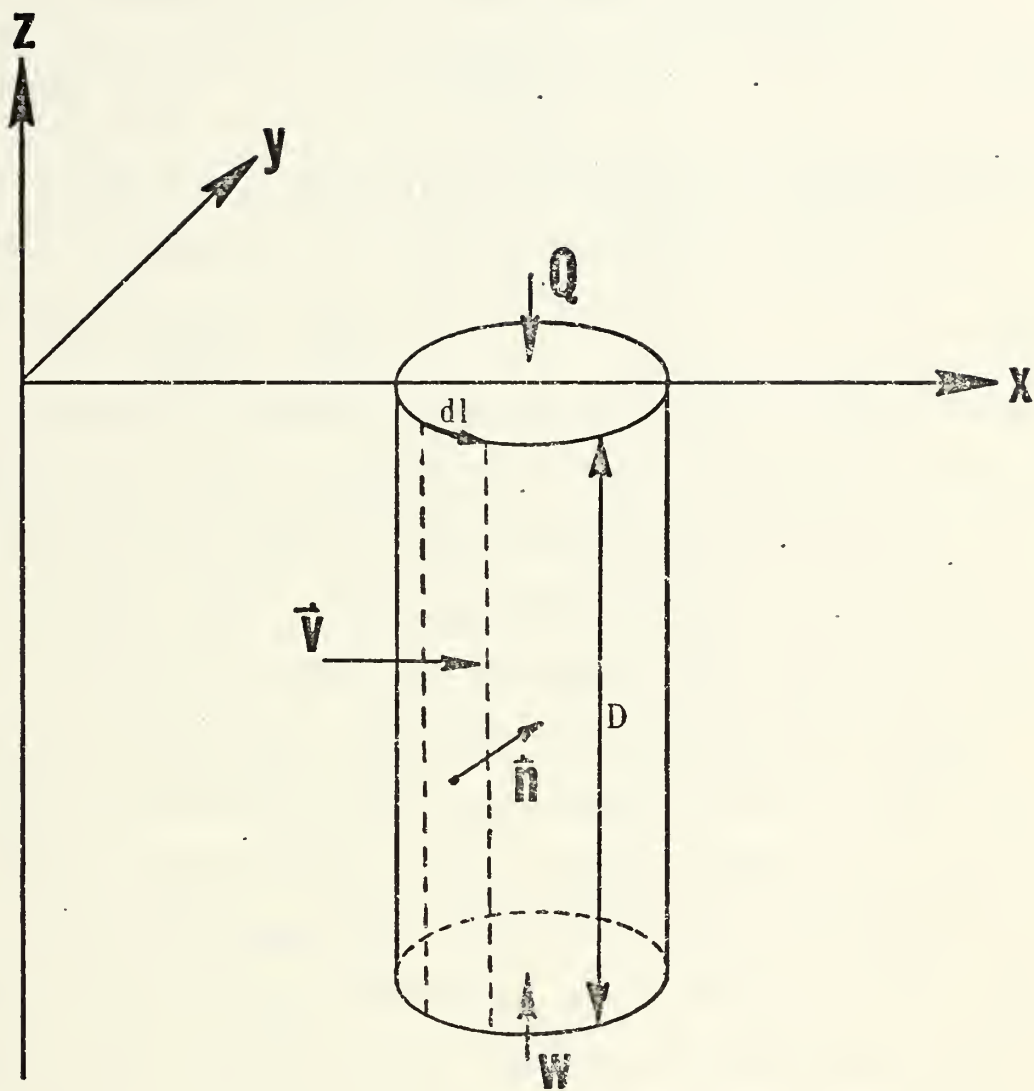


Figure 1. Notations used in the Heat Budget Equation.



$$\frac{\partial H}{\partial t} = - \frac{\partial}{\partial x} v^x H - \frac{\partial}{\partial y} v^y H + A^h \left( \frac{\partial^2 H}{\partial x^2} + \frac{\partial^2 H}{\partial y^2} \right) - \frac{1}{D} (wH - A \frac{\partial H}{\partial z}) + Q \quad (2)$$

(i)

(ii)

(iii)

(iv)

where the volume transports within the water column are defined by:

$$v^x = \frac{1}{D} \int_0^D u \, dz \quad v^y = \frac{1}{D} \int_0^D v \, dz \quad (3)$$

The vertical velocity,  $w$ , at depth  $D$  is obtained from the continuity equation expressed as the divergence of the velocity components in equation (3).

$$w = D \left( - \frac{\partial}{\partial x} v^x - \frac{\partial}{\partial y} v^y \right) \quad (4)$$

The left hand side of equation (2) is the local rate of change of total heat storage and the terms on the right hand side are the processes affecting the change in total heat storage. Seckel (1962) assumed the diffusion processes to be negligibly small, and the heat budget equation he used did not include terms (ii) and (iii). Wyrteki and Haberland (1968) analyzed the contribution of each term separately. Bathen (1971) extended his heat budget equation beyond the mixed-layer depth used by Seckel (1962) and Wyrteki and Haberland (1968) to a 250 m depth. Thus it could be assumed that the vertical processes of term (iii) balanced each other in this layer, and Bathen did not include them in his heat budget calculation. For the purposes of this study, and to systematically account for all the processes affecting the change in total heat storage, the first three terms on the right hand side of equation (2) representing advection and diffusion are treated as a single process. Hence, a simplified heat budget equation in which the local rate of change of total heat storage is balanced by the net heat flux at the air-sea interface and all processes occurring in the water column below the sea surface is written:

$$\frac{\partial H}{\partial t} = Q + \sum \text{sub-surface physical processes} \quad (5).$$



### III. SOURCES AND USAGE OF DATA

The values for each term in the simplified heat budget equation were computed using data readily available at FNWC. Computerized products provided the values of the required parameters at gridpoints of the standard FNWC 63 x 63 gridwork, which covers the Northern Hemisphere. The availability of monthly mean values suggested this as an appropriate time scale with which to begin the study, while the spatial scale was initially restricted to the 381 km gridpoint interval. The monthly mean values of the required oceanographic parameters were computed and stored between September 1971 and February 1975, and thus provided 41 sets of data.

Following Bathen (1971) the value of the total heat storage was calculated using the FNWC Sea-Surface Temperature, Potential Mixed-Layer Depth, and Sub-surface Thermal Structure analyses. An explanation of methods currently used at FNWC in producing these analyses is contained in Appendix A. Monthly values for the total heat storage were obtained by vertically integrating the temperature profile at each gridpoint from the surface to the standard 800 ft depth. This approximates the 250 m water column used by Bathen (1971), which is sufficiently deep to include all detectable seasonal variations of the thermal structure. Earlier heat budget studies by Seckel (1962) and Wyrтки and Haberland (1968) considered only the layer above the thermocline, assuming it to be highly stable for the time scales involved.

The monthly values of net heat flux across the sea surface were obtained from two FNWC products: Total Heat Exchange ( $Q_n$ ) Analysis and Total Heat Flux (THF) Analysis. Explanations of these are contained in Appendix A.





The final term in the simplified heat budget equation was the difference between the local change in total heat storage and the net air-sea heat flux.

A second source of data was the National Marine Fisheries Service (NMFS). For the past several years it has contracted merchant vessels to make expendable bathythermograph (XBT) soundings during ocean voyages. The frequency and regularity of transits between Hawaii and San Francisco have provided NMFS with an extensive amount of XBT data. Each transit was approximately four days in duration and permitted from 20 to 30 XBT soundings to be made at four-hour intervals. The availability of this data suggested that the initial analysis of FNWC data be restricted to a smaller 15 x 15 grid covering the eastern portion of the North Pacific Ocean. Based on the XBT profiles, NMFS calculated the values of total heat storage using an integration technique similar to the one used in this study for FNWC data. See Appendix C for an explanation of the computation scheme. The total heat storage was calculated for various layers including the 250 m layer. Interpolating the FNWC derived values from gridpoints to the great circle route and averaging the NMFS values to obtain monthly means permitted a comparison of the two sets of data. Net heat flux values for the eastern North Pacific prepared by Clark, et al. (1974) were also obtained from NMFS. These values were compared with the  $Q_n$  and THF values. An explanation of the method used by Clark et al. to compute the values of net heat flux is given in Appendix C.

The location of Ocean Weather Station (OWS) November along the great circle route at 30N, 140W provided a third source of data. The net heat flux computations by Dorman (1974) based on the OWS November data allowed a comparison with the FNWC values of net heat flux computed at the gridpoints adjacent to it.



#### IV. DISCUSSION OF RESULTS

It was the intent of this study to calculate a heat budget similar to Bathen (1971) for the eastern North Pacific Ocean using data available at FNWC. The reasons for calculating a heat budget were: 1) to determine if the monthly change in heat storage was balanced by the air-sea heat flux, 2) to determine the relative importance of the physical processes of advection and diffusion as factors accounting for the change in local heat storage. This determination would indicate whether changes in present mixed-layer models would be necessary before they can be tested on an ocean basin region. The procedure used here treated the processes of advection and diffusion as a singular process as noted in equation (5).

This section is divided into three parts. The first part begins with a description of the heat budget calculation using FNWC data, and then discusses examples of the calculation, focusing upon each term of equation (5). The second part investigates the air-sea heat flux term, comparing FNWC's  $Q_n$  fields to other computations of heat flux. The final part discusses the heat storage term computed from the FNWC temperature fields, and compares it with heat storage values obtained from NMFS XBT data.

##### A. EXAMPLES OF THE HEAT BUDGET CALCULATION

The purpose of the heat budget calculation was to determine the relative importance of each term on the right hand side of equation (5). The first step was to determine the local rate of change of total heat storage. The total heat storage was computed by integrating the monthly mean values of sea surface temperature and temperatures at 100, 200, 300, 400, 600, and



800 feet. These data were used directly from the FNWC files of monthly means for the months September 1971 through February 1975. The local rate of change of total heat storage was then computed by subtracting the value of total heat storage for one month from the value for the succeeding month. The difference, or change in heat storage per month, reflects the 30-day period from the 15th of one month to the 15th of the next month. Positive values of change in heat storage indicate a gain in total heat storage while negative values indicate a loss.

The second step involved computing the values of air-sea heat flux for the corresponding 30-day period. FNWC computes a bi-monthly mean of the  $Q_n$ . Values for the last half of each month were added to the values for the first half of the next month in this study. Positive values of  $Q_n$  represent a downward heat flux to the ocean and negative values represent an upward heat flux to the atmosphere.

The final step in the heat budget calculation was to determine the values of the subsurface physical processes, namely horizontal advection and diffusion. Rearranging the terms in equation (5):

$$\sum \text{subsurface physical processes} = \frac{\partial H}{\partial t} - Q \quad (6)$$

For the purposes of this study the left hand side of equation (6) is termed a "residual." Over a 30-day period small positive or negative values indicate that the change in total heat storage is balanced by the air-sea heat flux. Larger values indicate that subsurface physical processes also play a role in balancing the change in total heat storage.

It will be shown in the second part of this section that a reasonable value of heat flux, upward or downward, is  $4.5 \text{ kcal cm}^{-2}$  or less for a 30-day period. This is equivalent to a heat flux value of  $150 \text{ cal cm}^{-2} \text{ day}^{-1}$ .



Thus the change in heat storage should be close to that value if the heat flux is to balance it. This is a basic hypothesis upon which mixed-layer models have been developed. Small errors in the temperature values used to compute the heat storage term will produce significant errors in the total heat storage. For a given sounding of 250 m, a bias of  $0.5^{\circ}\text{C}$  through the column would produce an error of  $12.5 \text{ kcal cm}^{-2}\text{mo}^{-1}$ . As described in Appendix A, the Subsurface Thermal Structure Analysis is heavily dependent upon the Sea Surface Temperature Analysis to produce quasi-synoptic fields. Furthermore, positive gradients in the thermal structure are permitted at only a few selected gridpoints. Thus the temperature values along a forced negative gradient reflect any bias in the sea-surface temperature. Hopefully, the objective spatial analysis schemes, discussed in Appendix B, and the time averaging of 60 or more analyses each month would reduce this error. A bias of  $0.2^{\circ}\text{C}$  averaged over a 250 m water column would produce an acceptable error in heat storage of  $5 \text{ kcal cm}^{-2}\text{mo}^{-1}$ .

Although the heat budget calculation was performed for 41 sets of data, the following discussion is centered upon two 30-day periods in 1974. The first one was during the seasonal heating period of the eastern North Pacific Ocean and covers from 15 June to 15 July. The second period was from 15 November to 15 December during the cooling season. These periods in 1974 were chosen because of the availability of a second source of heat flux data at FNWC; the Total Heat Flux (THF) which has been stored only since June 1974.

Figure 2 is a representation of the change in total heat storage values computed at 225 gridpoints covering the eastern North Pacific. The heat storage values are calculated over 250 m column and are analyzed at  $10 \text{ kcal cm}^{-2}\text{mo}^{-1}$  intervals. For the period 15 June to 15 July, the gain in total heat storage exceeds  $10 \text{ kcal cm}^{-2} \text{ mo}^{-1}$  north of  $20^{\circ}\text{N}$ . This represents an





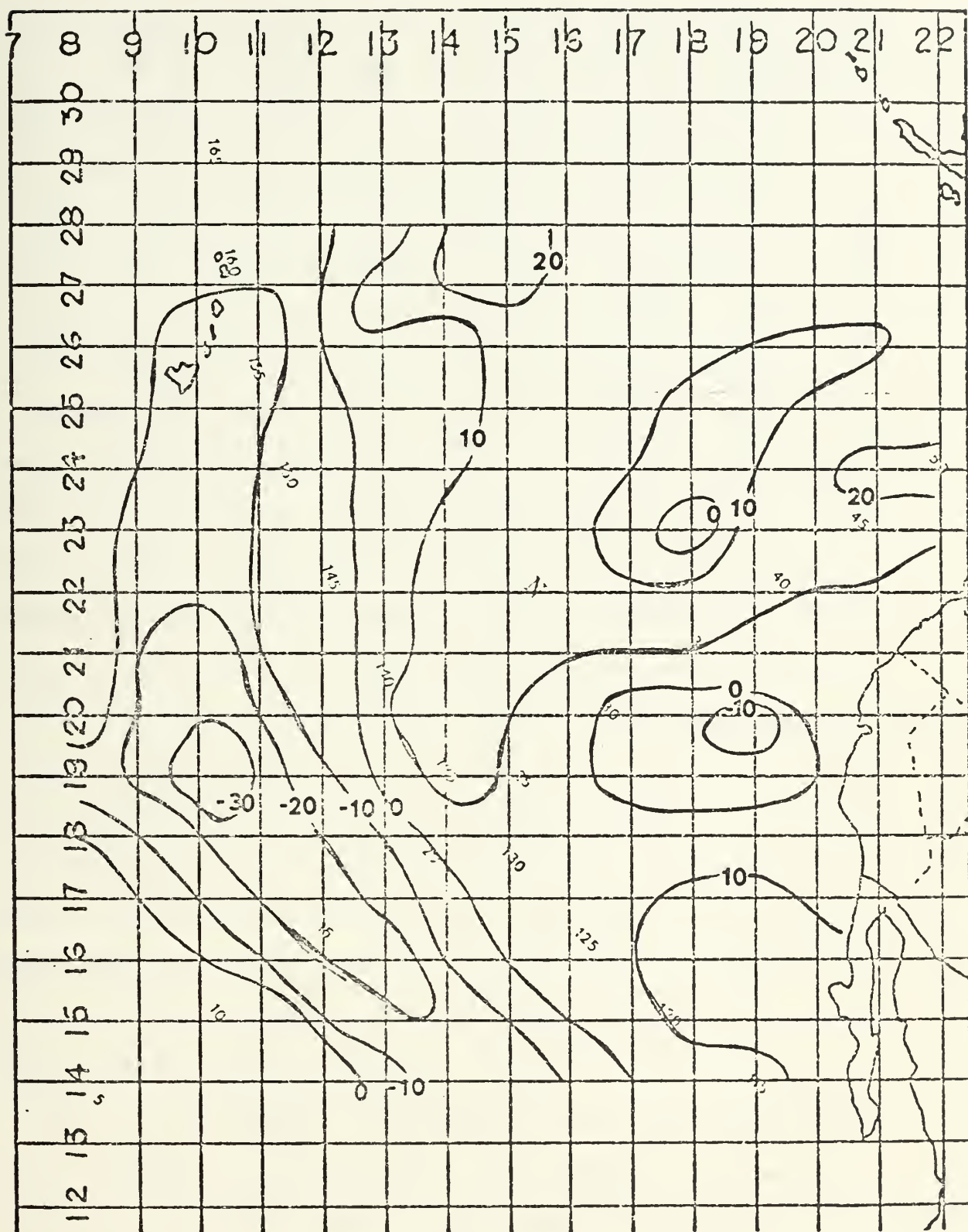


Figure 2. Heat Storage Change--15 June to 15 July 1974



average temperature increase of  $0.4^{\circ}\text{C}$  throughout the 250 m water column. South of 20N a loss in total heat storage occurred during the period. Values exceed  $30 \text{ kcal cm}^{-2} \text{ mo}^{-1}$  over a considerable area in that region. At this latitude each grid square covers an area of 27,000 square miles.

Figure 3 is an analysis of the values of heat flux for the same period. Characteristic of the heating season, all values are positive, and exceed  $15 \text{ kcal cm}^{-2} \text{ mo}^{-1}$  over most of the eastern North Pacific. A large area off the west coast of the United States exceeds  $20 \text{ kcal cm}^{-2} \text{ mo}^{-1}$ .

The difference between the two figures is depicted in Figure 4 and represents the subsurface physical processes or residual term of equation (6). North of 20N, the gain in total heat storage depicted in Figure 2 was not completely balanced by the heat flux shown in Figure 3. The excessive downward heat flux was evidently balanced by physical processes of advection and diffusion. Over most of the region, the magnitude of these processes is less than half that of the heat flux. However, off the California coast and near 40N, 140W the magnitude of the residual term is equal to, or exceeds, the corresponding values of heat flux by  $10 \text{ kcal cm}^{-2} \text{ mo}^{-1}$ . South of 20N the residual term is two to three times larger than the heat flux term. The advection and diffusion pattern of Figure 4 is similar to the heat storage change pattern of Figure 2, except the values are 10 to  $20 \text{ kcal cm}^{-2} \text{ mo}^{-1}$  greater. The large negative values have compensated for the downward heat flux and loss in total heat storage.

Figure 5 is the analysis of the values of heat storage change for the period 15 November to 15 December 1974. The expected loss of heat has occurred over most of the region. Three areas north of 20N, and a large area south of 20N, have shown a gain in heat storage during this period.



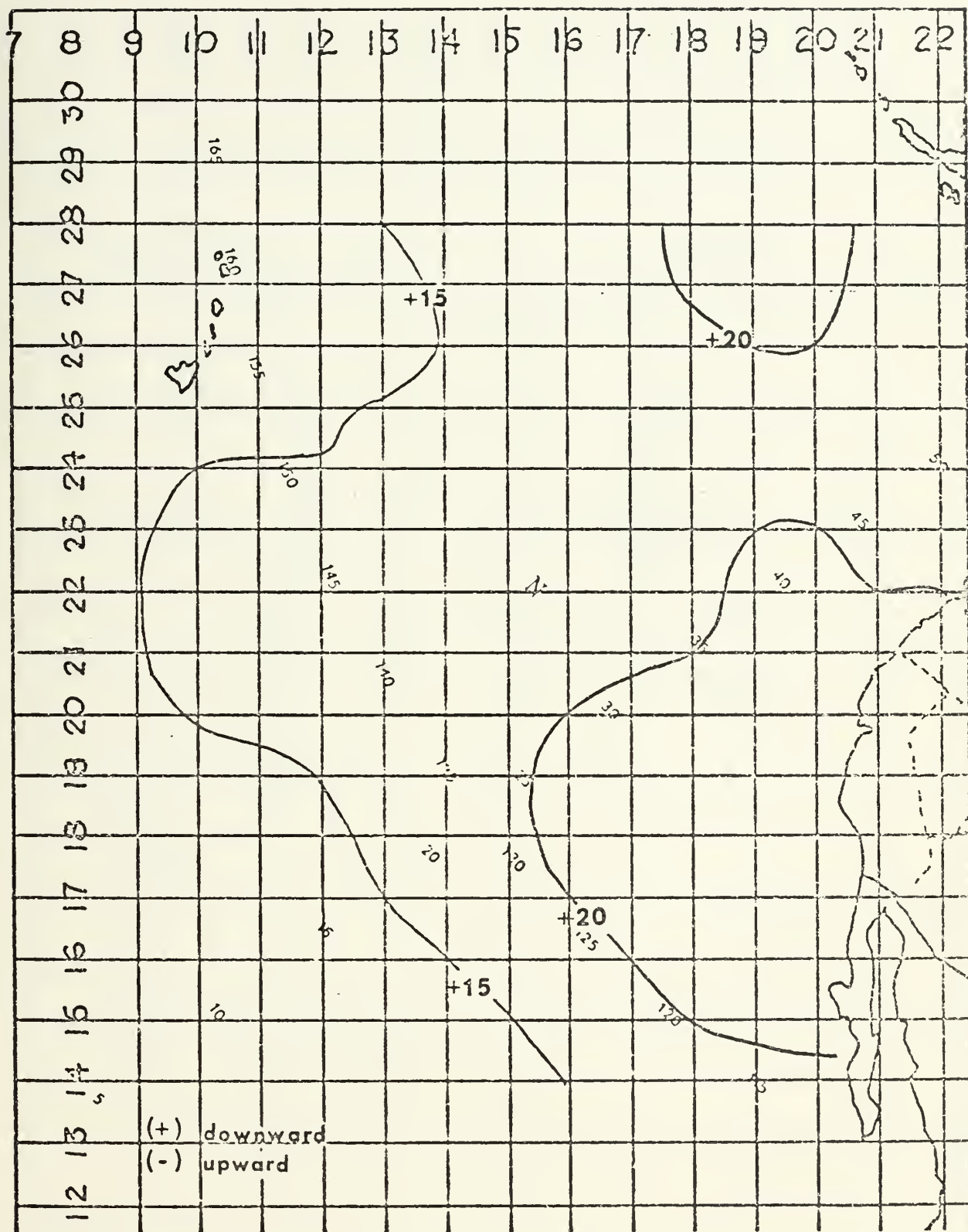


Figure 3. Total Heat Exchange ( $Q_n$ ) analysis--15 June to 15 July 1974





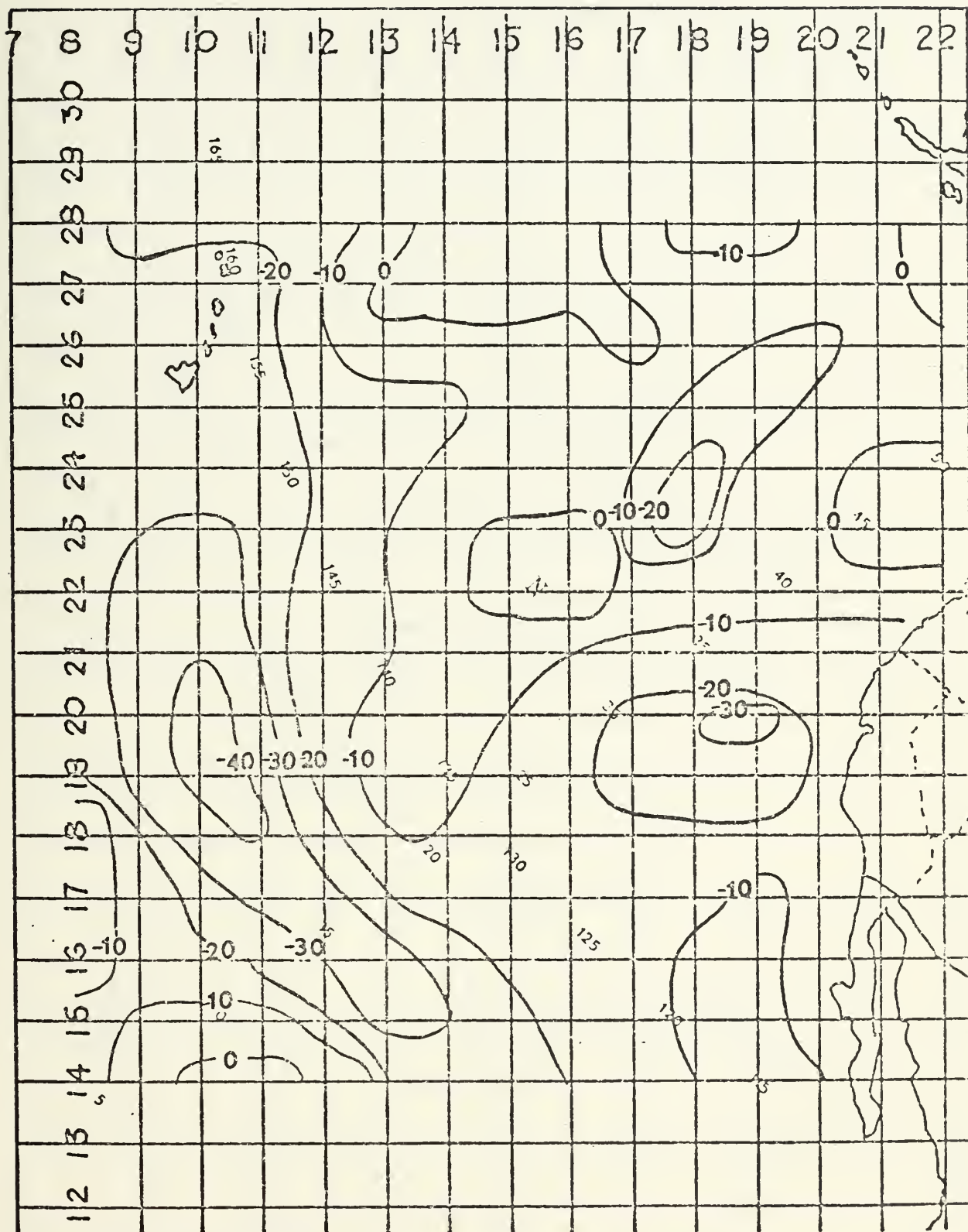


Figure 4. Computed Residual Using  $Q_n$  Values of Heat Flux  
15 June to 15 July 1974





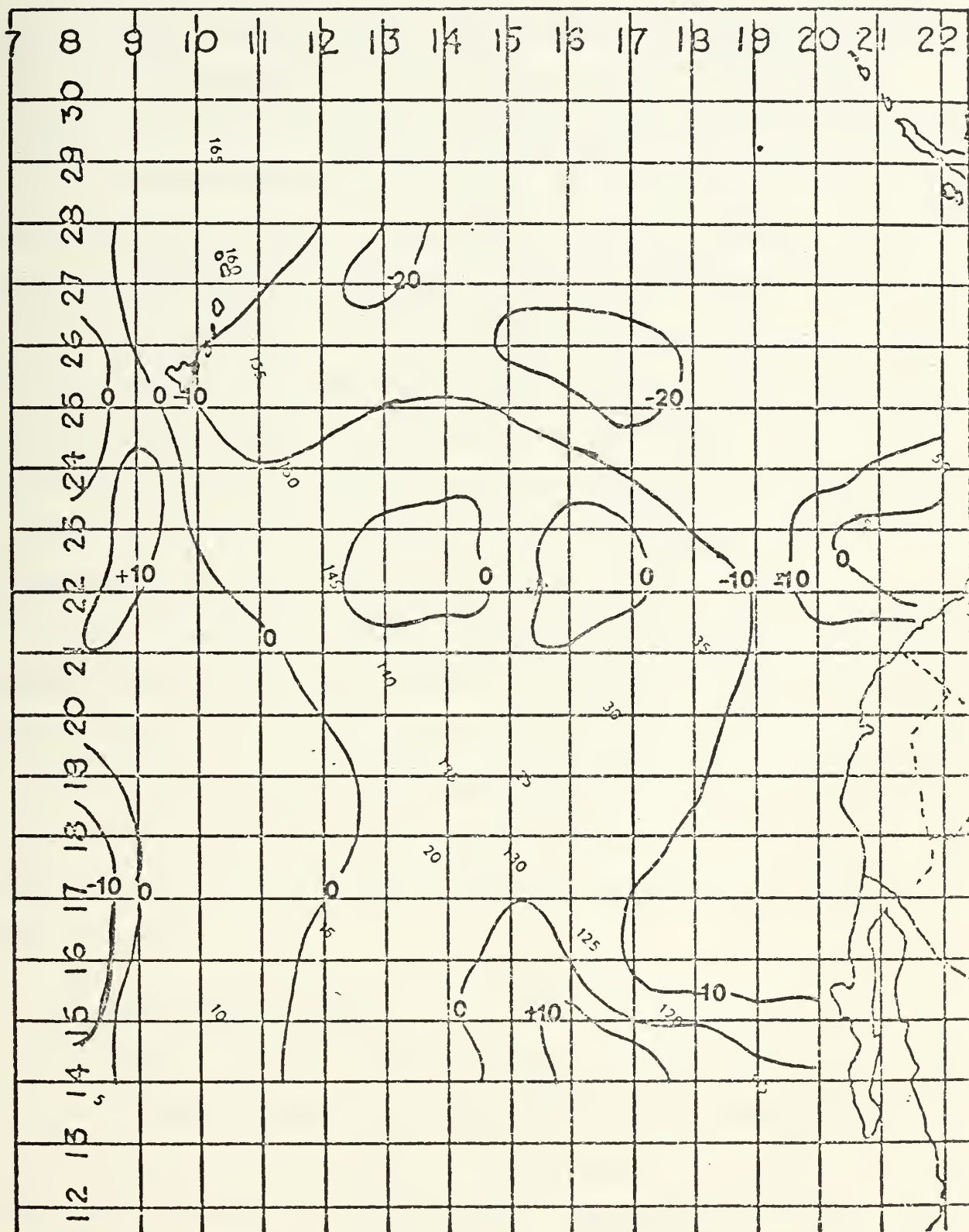


Figure 5. Heat Storage Change--15 November to 15 December 1974



The net heat flux for this period is shown in Figure 6. A slight upward flux of heat has occurred north of 30N and along the California coast. In other areas a downward flux of heat to the ocean still occurs during the cooling season, although the values are generally less than  $5\text{kcal cm}^{-2} \text{ mo}^{-1}$ .

The residual field depicted in Figure 7 is quite similar to the heat storage change field of Figure 5. In this case the near-zero values of the heat flux did not balance the loss of heat. Apparently, advection and diffusion account for the change in heat storage that has occurred. Significant advection can occur in the stronger oceanic current systems, such as the western boundary current systems or the equatorial current systems. Cases of anomalous oceanic conditions produced by advection are normally a result of warmer water being advected into a colder region. The examples presented above indicate advection of colder water into the regions of heat loss.

A perfect balance of the heat storage term by the heat flux term was not expected over the entire area. However, the significant deviations in some areas for the two examples presented above suggested the possibility of errors in one or both of the terms. The examples presented above are typical of the 41 months studied in this heat budget calculation. The following two parts of this section investigate, separately, the heat flux term and the heat storage term.

## B. AIR-SEA HEAT FLUX TERM

Since air-sea interaction processes cannot, in general be measured directly except for solar radiation, for which there are limited measurements over the oceans, quantitative evaluation of these processes depends upon computations based on empirically derived formulas. These formulas are still the subject of extensive research, and heat exchange computations are considered



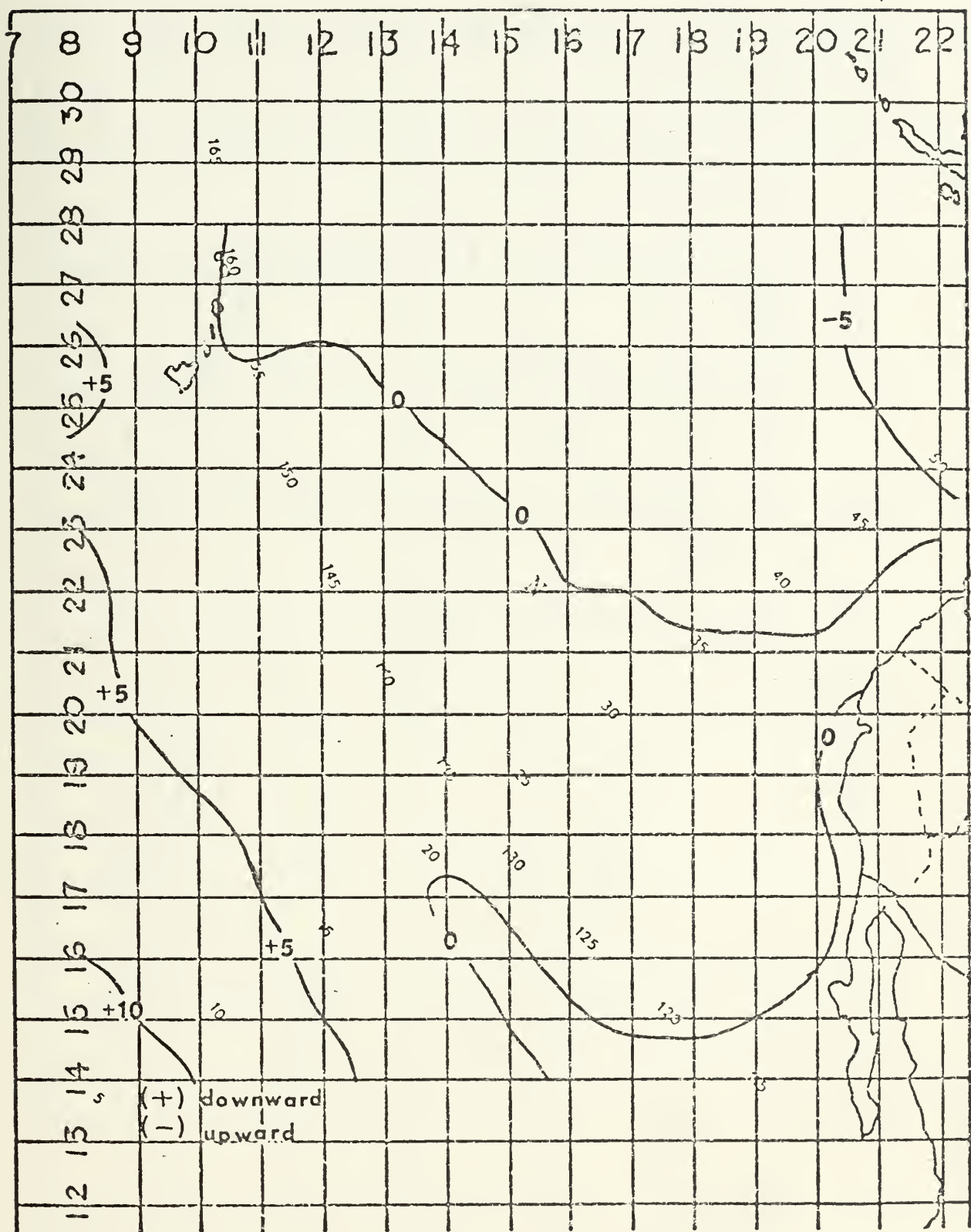


Figure 6. Total Heat Exchange ( $Q_n$ ) Analysis--15 November to 15 December 1974





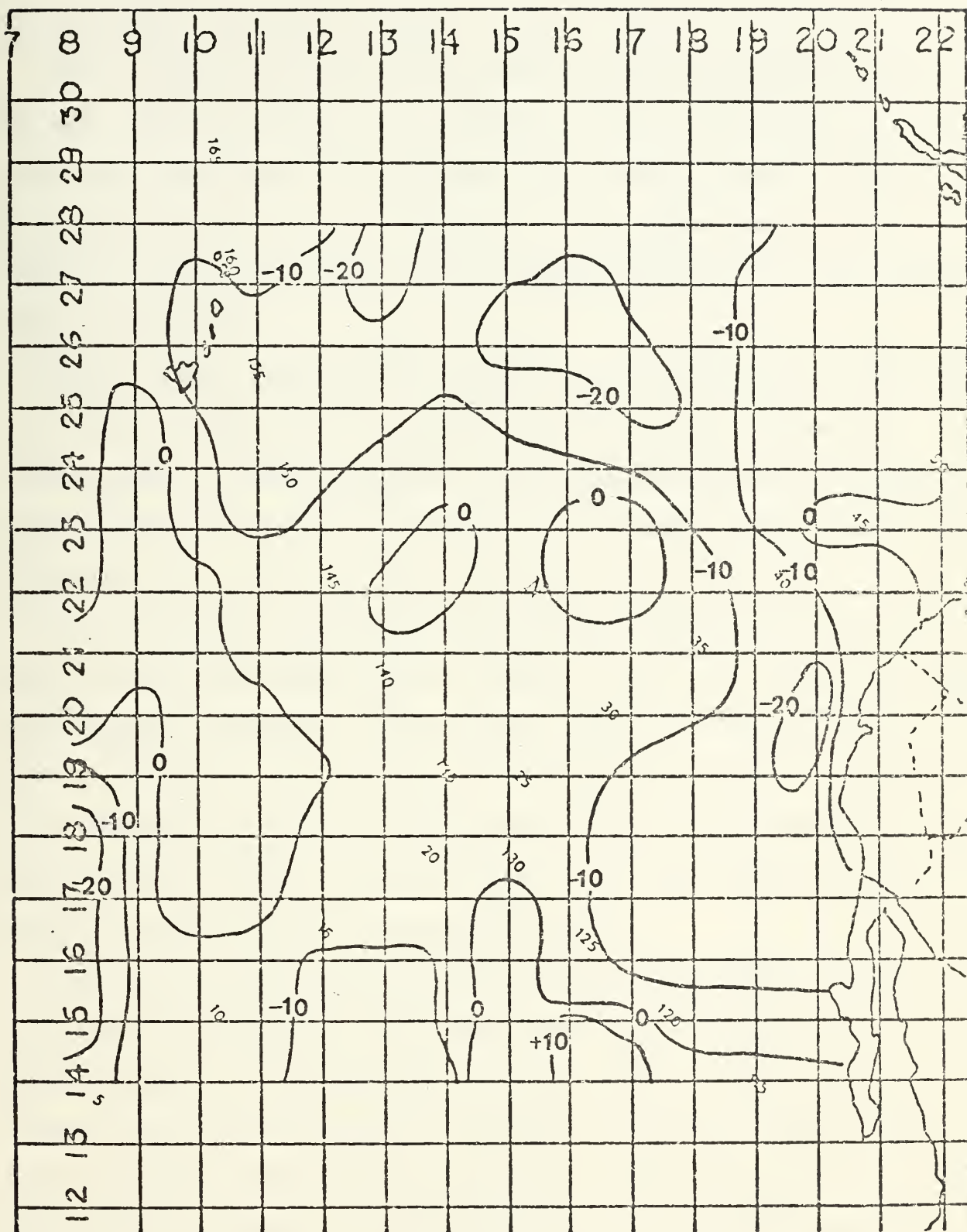


Figure 7. Computed Residual Using  $Q_n$  Values of Heat Flux  
15 November to 15 December 1974





only as relative indices of the magnitude of the heat flux across the air-sea interface. (Clark et al., 1974)

FNWC had computed bi-monthly mean values of Total Heat Exchange,  $Q_n$ , for the same time series of data used to compute the total heat storage in the heat budget calculation. A description of the empirical equations used to derive values of  $Q_n$  is given in Appendix A. These values were used in the initial heat budget computation with the examples presented in the preceding part of this section.

Another computation of the air-sea heat flux called Total Heat Flux (THF), was available at FNWC. As it is derived from the atmospheric primitive-equation model, it should represent a considerable improvement over the empirically derived values of  $Q_n$ . A description of this FNWC product is also given in Appendix A.

Figure 8 compares four different computations of air-sea heat flux at Ocean Weather Station (OWS) November located at 30 N, 140 W. The graph shows close agreement between the long term means computed by Dorman (1974) and Clark et al. (1974). The formulas used by Clark et al. are given in Appendix C. Although the 1974 monthly mean values of THF at OWS November deviate from the ten-year means of Dorman and Clark et al., they represent a more plausible anomaly than the corresponding  $Q_n$  values.

Figure 9 is an analysis of the heat flux values derived by Clark et al. (1974) for 5 degree squares in the eastern North Pacific north of 20 N. The period covered by the long-term mean is from 15 June to 15 July. The corresponding THF analysis from 1974 is presented in Figure 10. The two analyses are generally similar, and are quite different from the  $Q_n$  field for this time as shown in Figure 3. Of particular note is the area of upward heat flux near 20 N. Figures 11 and 12 are the analyses of heat flux from Clark et al. (1974) and FNWC THF for a 30-day period in the cooling season.



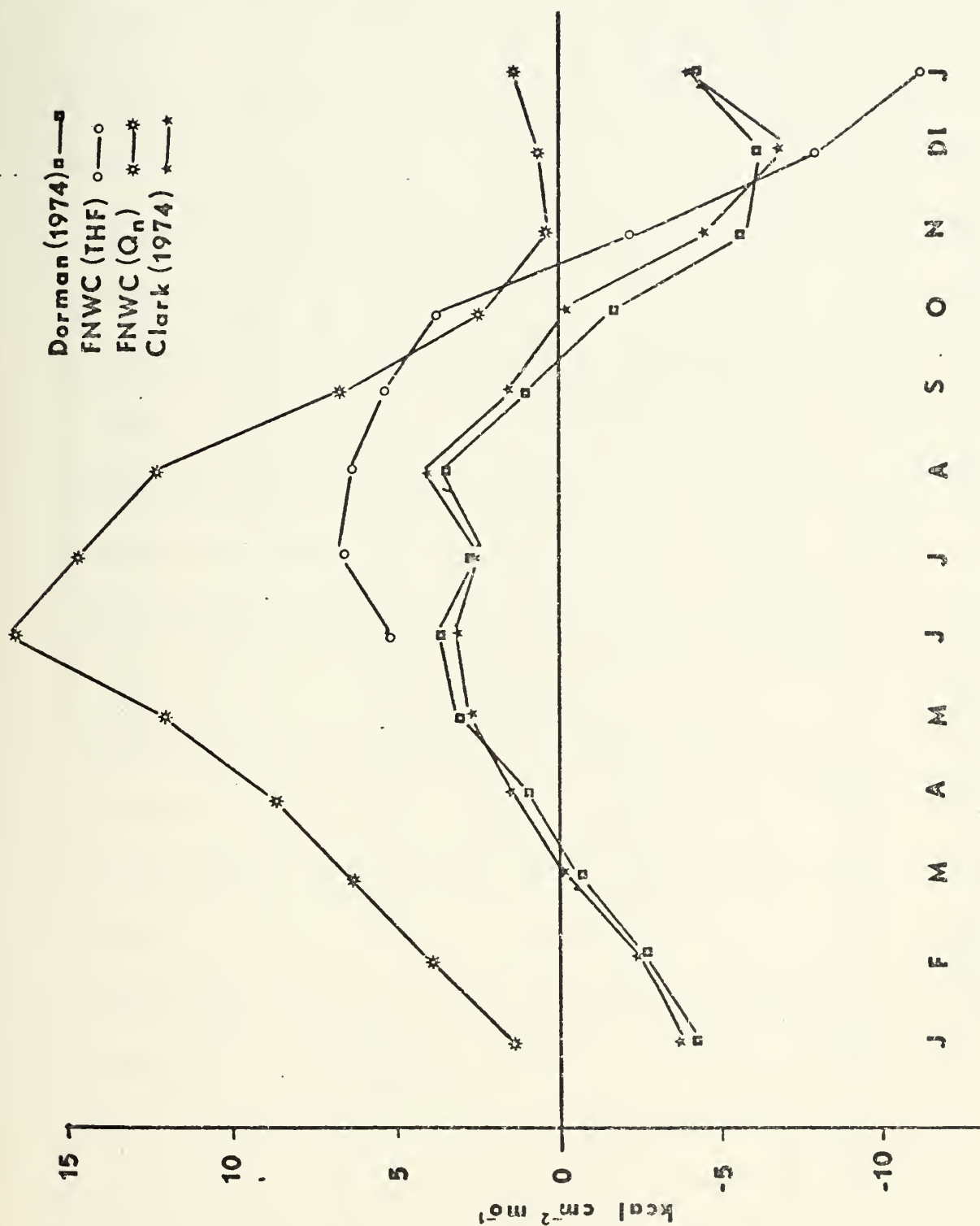


Figure 8. Comparison of Heat Flux Values at OWS November.



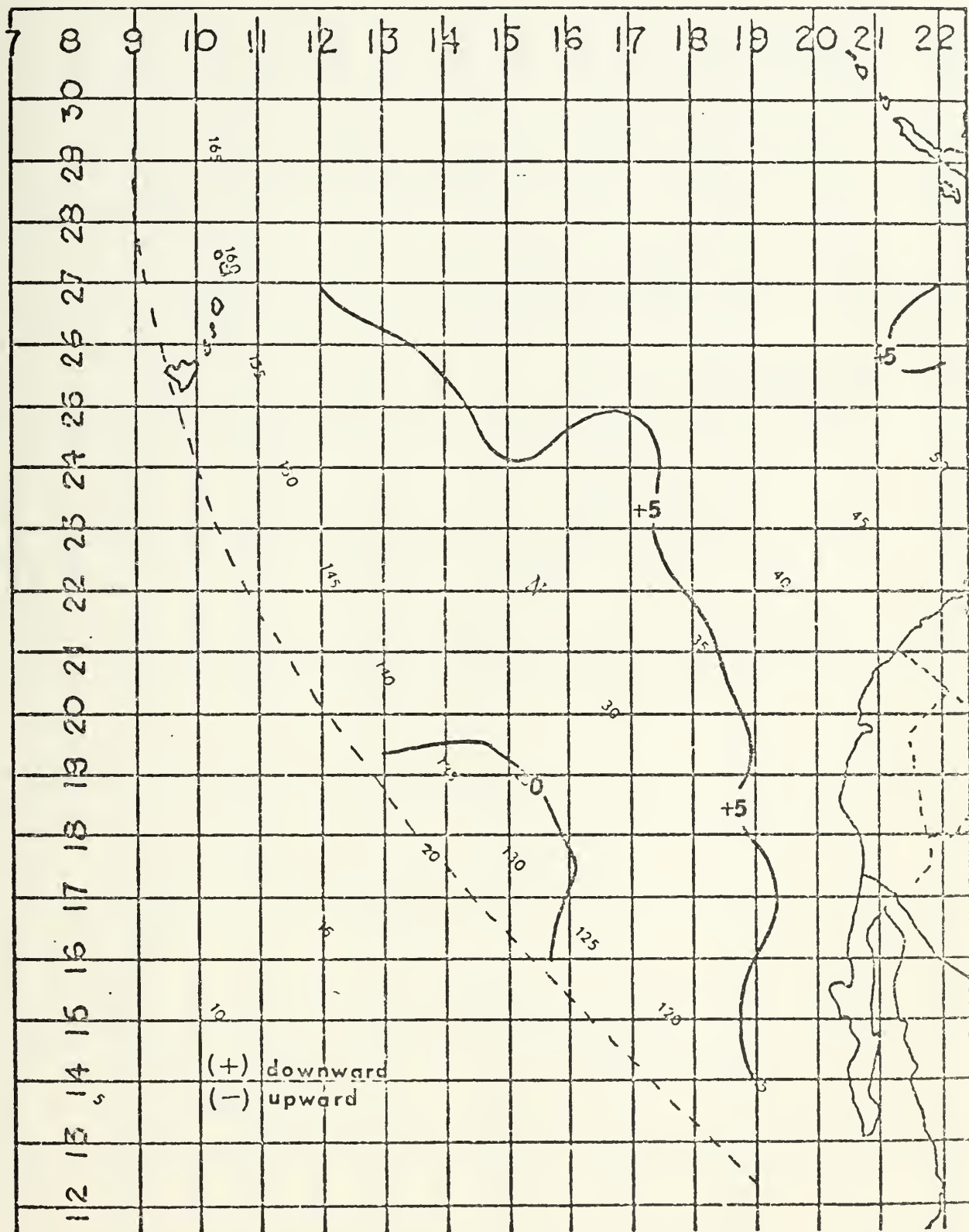


Figure 9. 1961-1971 Mean Net Heat Flux Derived by Clark et al. (1974)  
for 15 June to 15 July



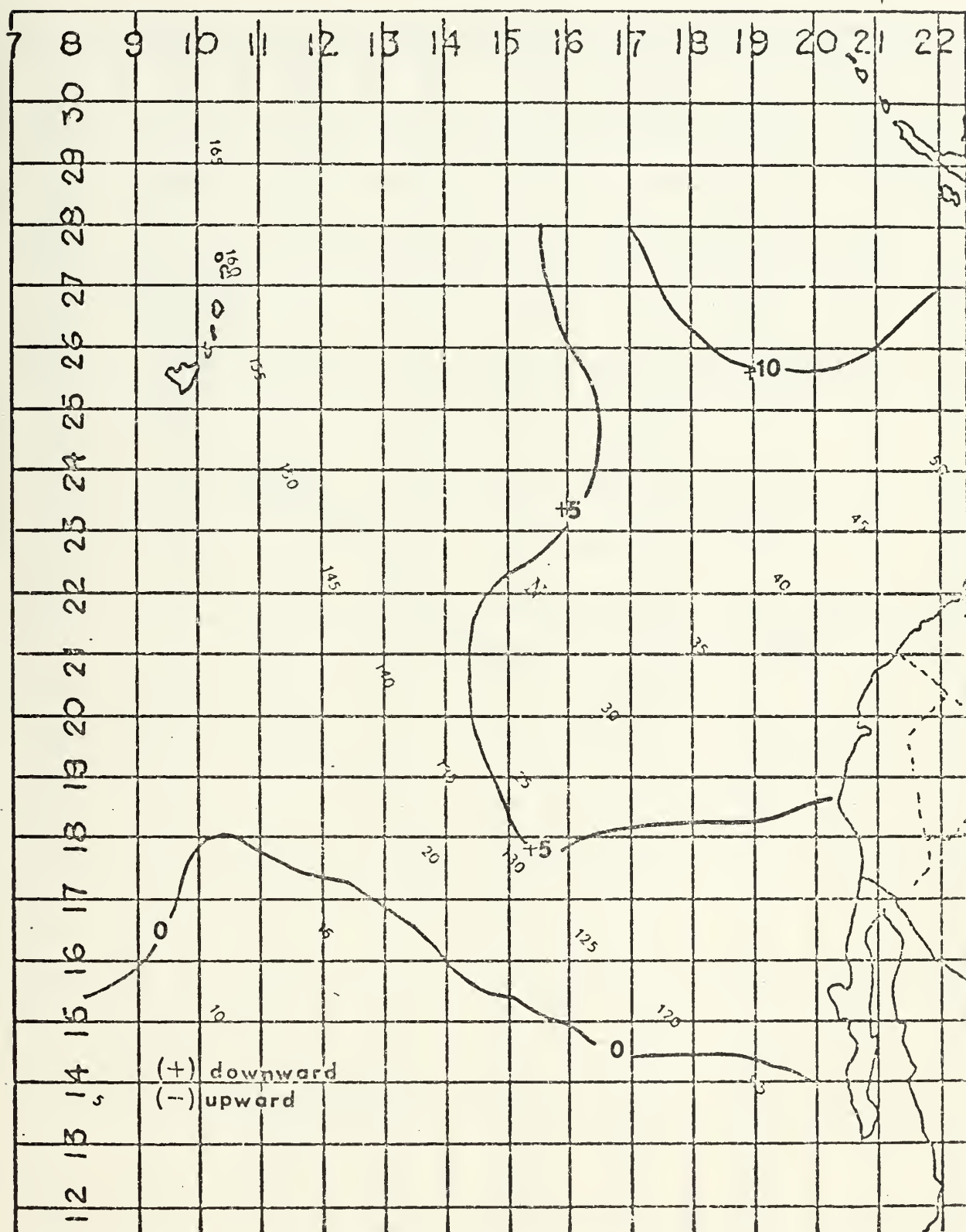


Figure 10. Total Heat Flux (THF) Analysis--15 June to 15 July 1974









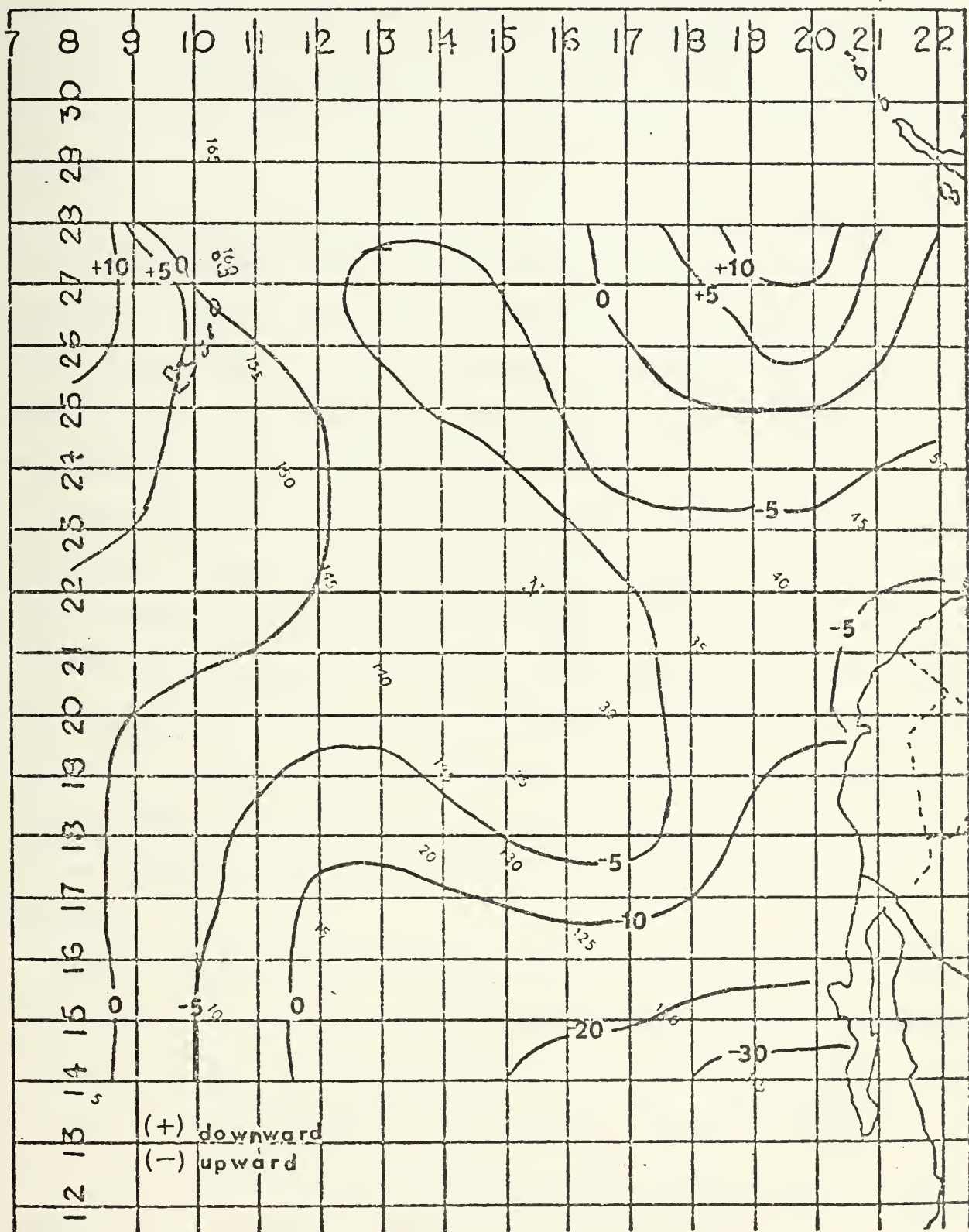


Figure 12. Total Heat Flux (THF) Analysis--15 November to 15 December 1974



Figure 12 should also be compared with the  $Q_n$  analysis in Figure 6. Areas of large upward heat flux from the ocean appear off Baja California on the THF analysis. In addition, a  $10 \text{ kcal cm}^{-2} \text{ mo}^{-1}$  area of downward heat flux shows up in the Gulf of Alaska throughout the heating season and into the cooling season.

The heat budget calculation, comparable to those shown in Figures 4 and 7, was repeated using the THF values instead of the  $Q_n$  values for the heat flux term. Since the THF fields have only been stored by FNWC since June of 1974, the heat budget could only be examined using eight monthly means of heat flux data. For purposes of comparison the examples below cover the same periods in 1974 that were previously presented.

Figure 13 is the analysis of the residual term for the period 15 June to 15 July. The small values of heat flux shown in Figure 10 have not balanced the change in heat storage shown in Figure 2. In fact, the residual field is nearly identical to the change in heat storage field. Again large negative residual values exceeding  $20 \text{ kcal cm}^{-2} \text{ mo}^{-1}$ , south of 20 N, indicate a loss in heat storage caused by processes other than upward heat flux from the ocean. In addition, positive residual values exceeding  $10 \text{ kcal cm}^{-2} \text{ mo}^{-1}$  indicate a gain in heat storage by processes of advection and diffusion.

Figure 14 is the residual field from the period 15 November to 15 December. Referring to Figure 5, little or no change in heat storage has occurred in a large central area of the analysis. The correspondingly small values of upward heat flux in Figure 12 have essentially balanced the change in heat storage. However, the large negative residual values in the Gulf of Alaska reflect the anomalous downward heat flux seen in Figure 12. South of 20 N the positive residual values are equal in magnitude to the negative values of heat flux. This suggests that advection and diffusion processes





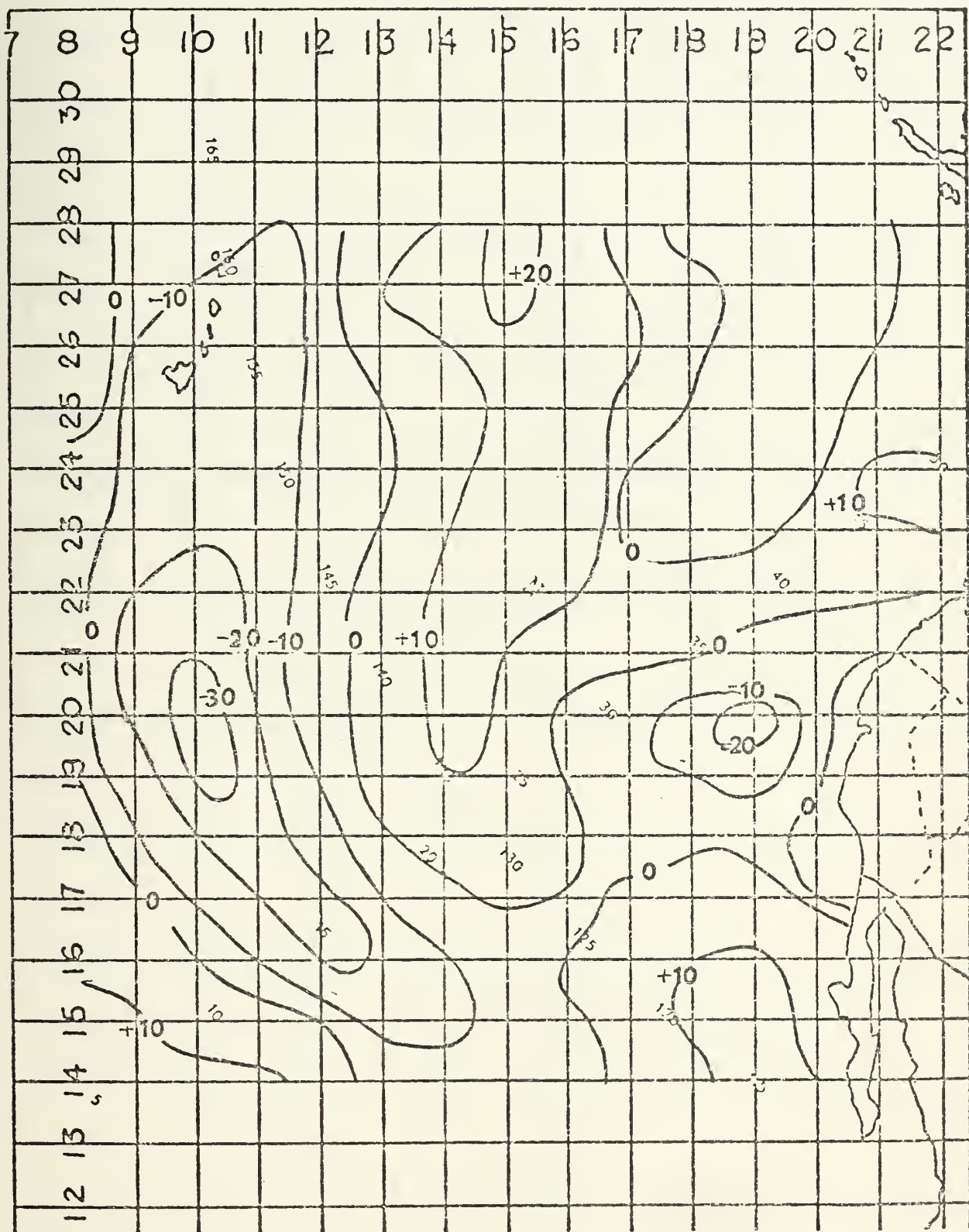


Figure 13. Computed Residual Using THF Values of Heat Flux--  
15 June to 15 July 1974





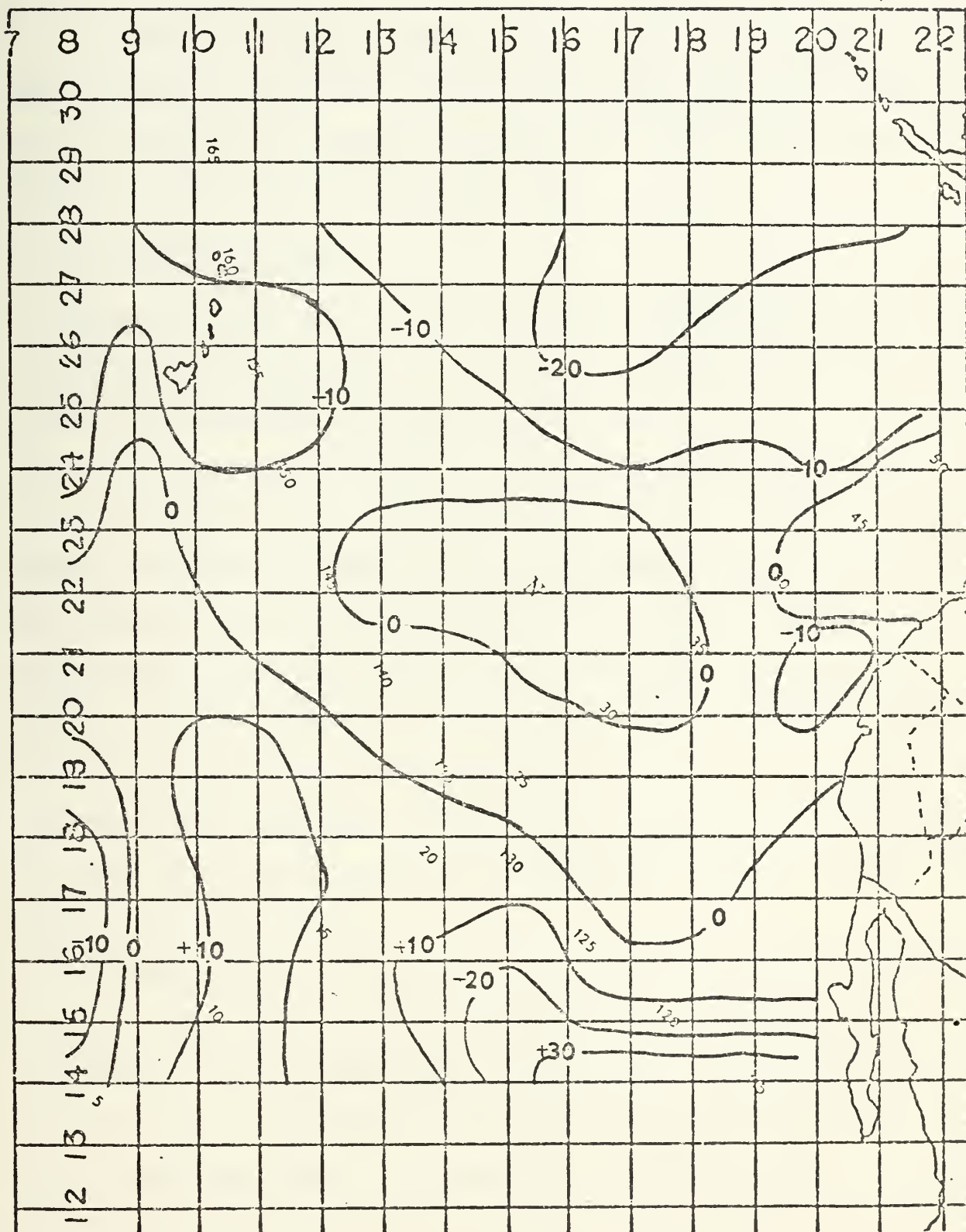


Figure 14. Computed Residual Using THF Values of Heat Flux--  
15 November to 15 December 1974



tending to produce a gain in heat storage were balanced by the upward heat flux from the ocean.

In summary, a second heat budget calculation was made using considerably improved values of heat flux. The resulting residual fields were comparable to the residual fields computed in the first heat budget. The next part of this section discusses the heat storage term.

### C. THE HEAT STORAGE TERM

The heat storage term was calculated directly from the FNWC monthly mean temperatures in the upper 250 m of the ocean. In a previous section it was pointed out that biases in the temperatures at each of the standard levels can result in significant changes in the heat storage for a given 30-day period. A monthly change of more than  $0.2^{\circ}\text{C}$ , averaged over the 250 m water column, will result in a heat storage change greater than  $5\text{ kcal cm}^{-2}\text{ mo}^{-1}$ . The values of heat flux shown in Figures 9 and 10 indicate that this term alone cannot balance larger changes in the heat storage. Thus, if large changes in the heat storage are assumed to be realistic, physical processes of advection and diffusion become important. In this section the heat storage term will be investigated to see if large changes can be realistically attributed to physical processes or to computational errors in the data fields used to compute them.

The first approach taken in this investigation was to compare temperature profiles constructed from the data fields used in the computation of the heat storage term. The long-term or climatological, and monthly mean profiles for June, July and August of 1974 are given in Figures 15 to 18. Figures 15 and 16 were taken from gridpoints adjacent to OWS November. Extensive BT data should have been available from this location for use in the Subsurface Thermal Structure Analyses as described in Appendix A. Figures 17 and 18



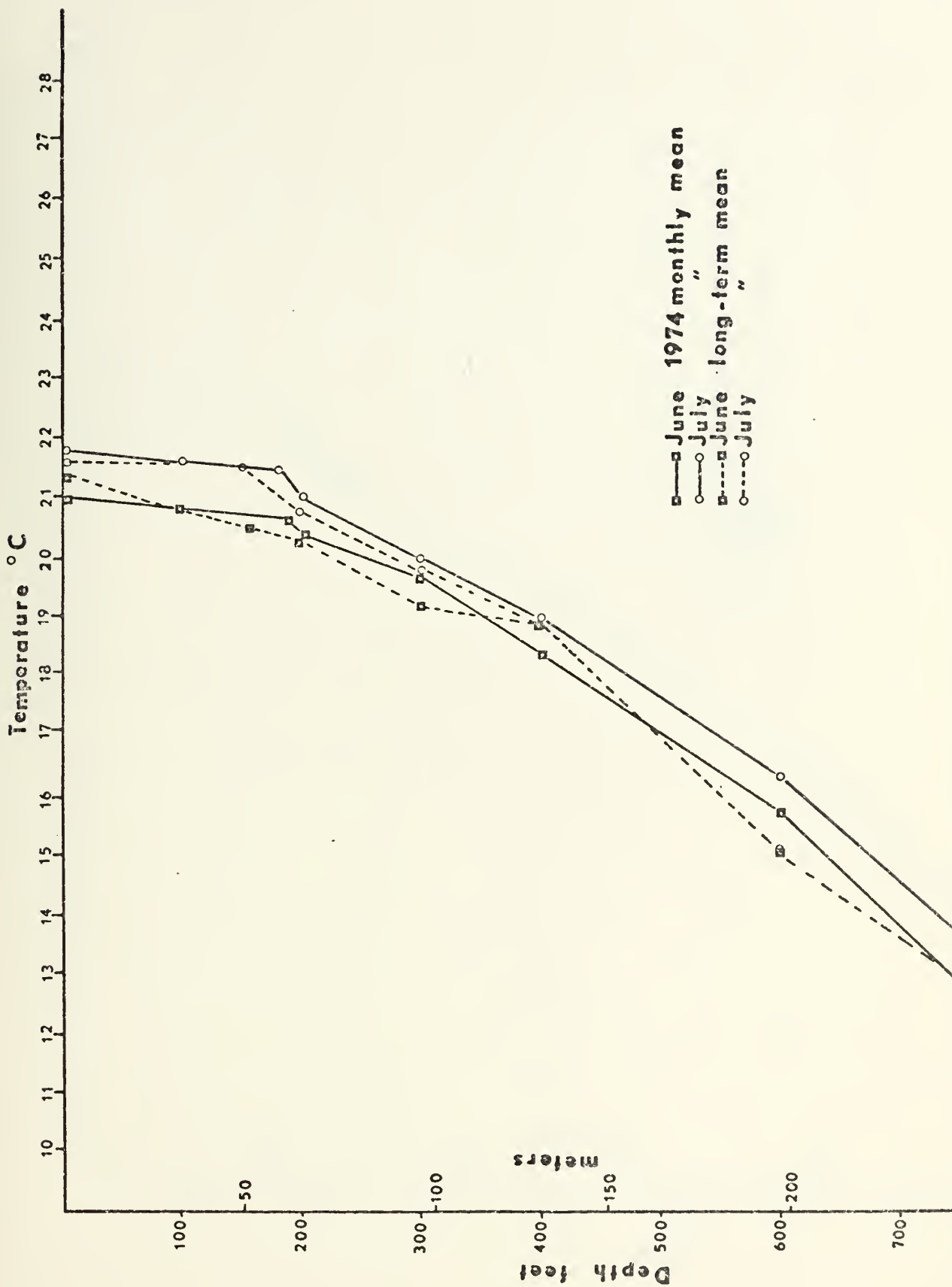


Figure 15. 1974 Monthly Mean and Long-Term Mean Temperature Profiles for June and July near OWS November



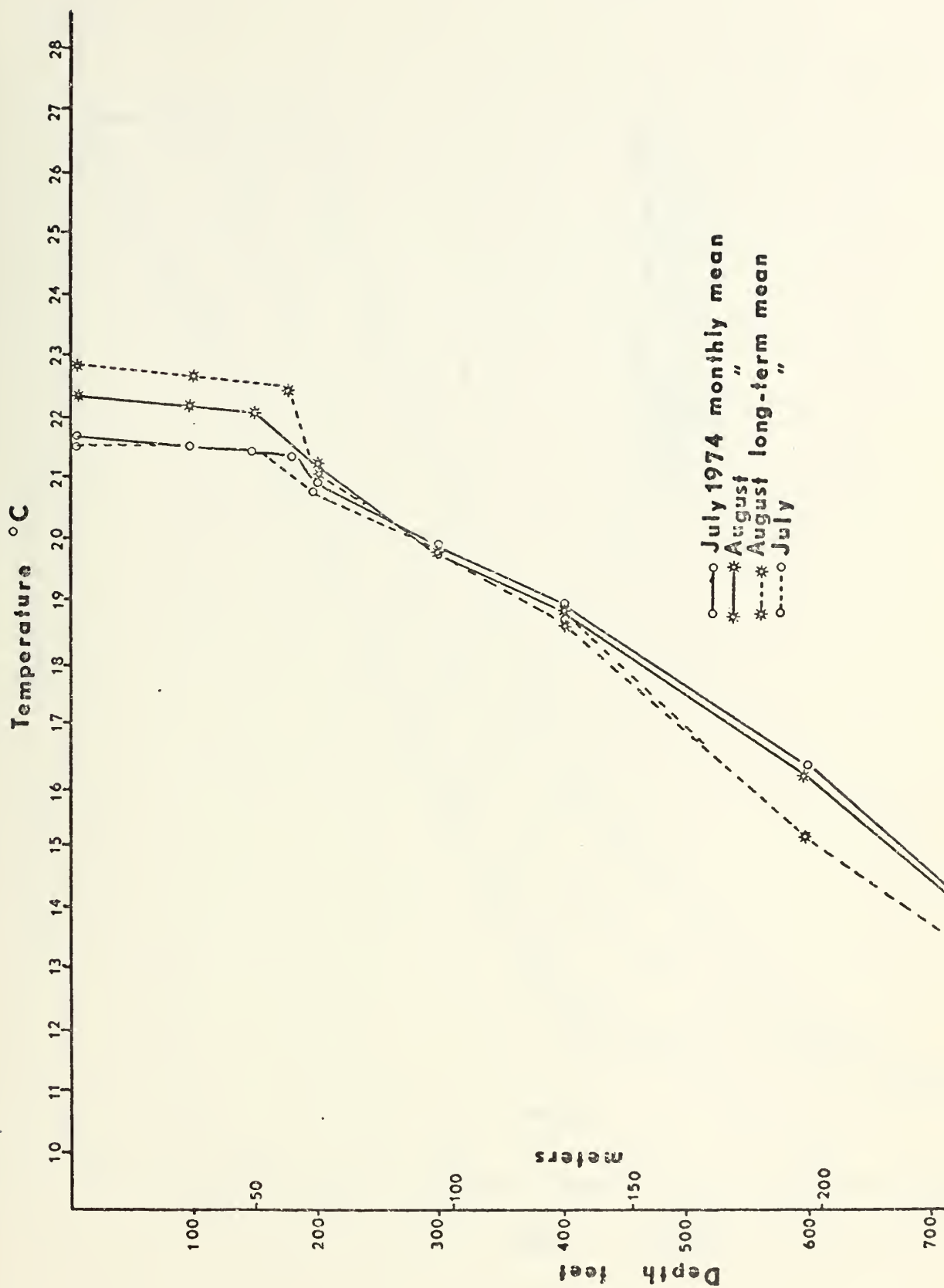


Figure 16. 1974 Monthly Mean and Long-Term Temperature Profiles for July and August near OWS November





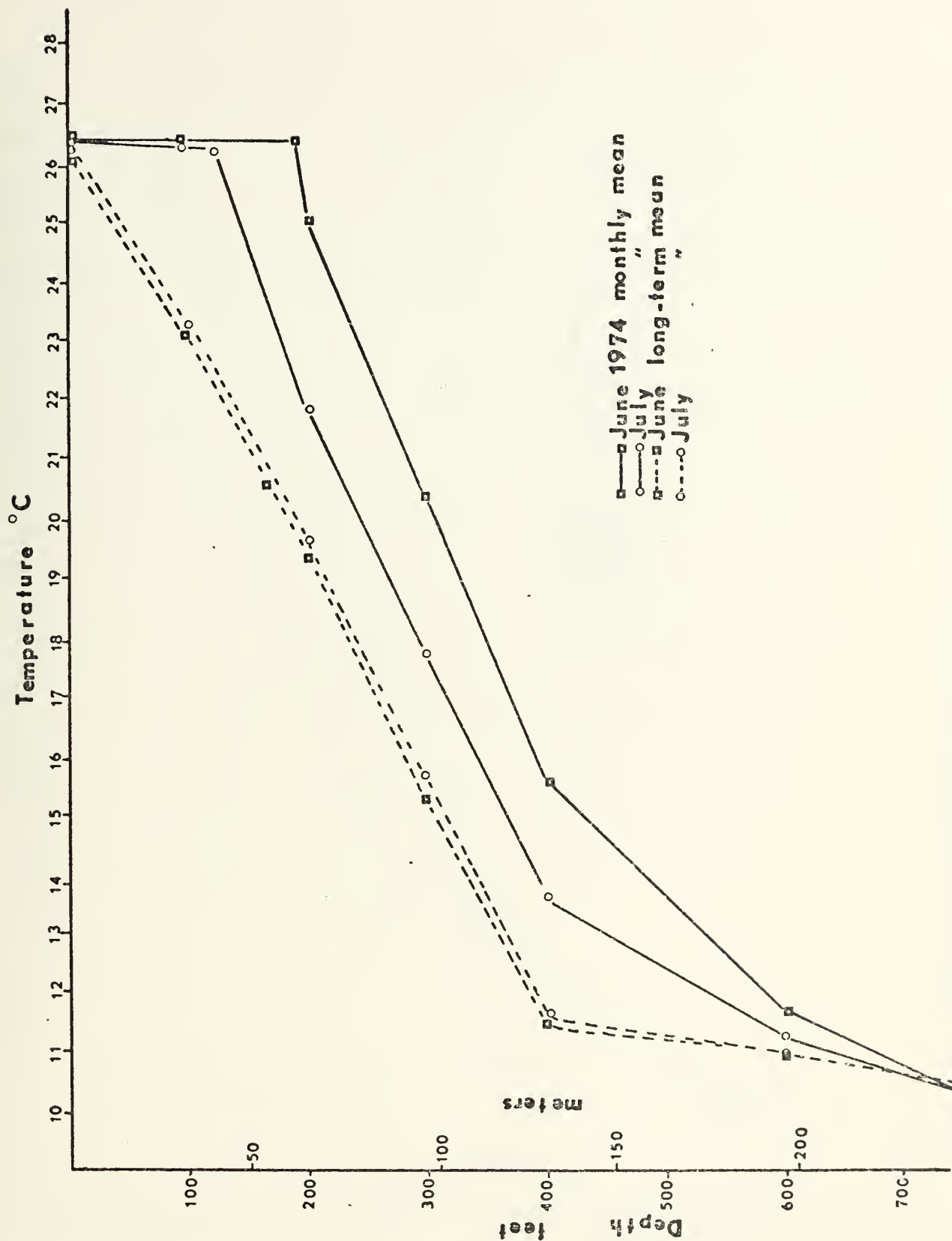


Figure 17. Monthly Mean and Long-Term Temperature Profiles for June and July near 15N, 140W



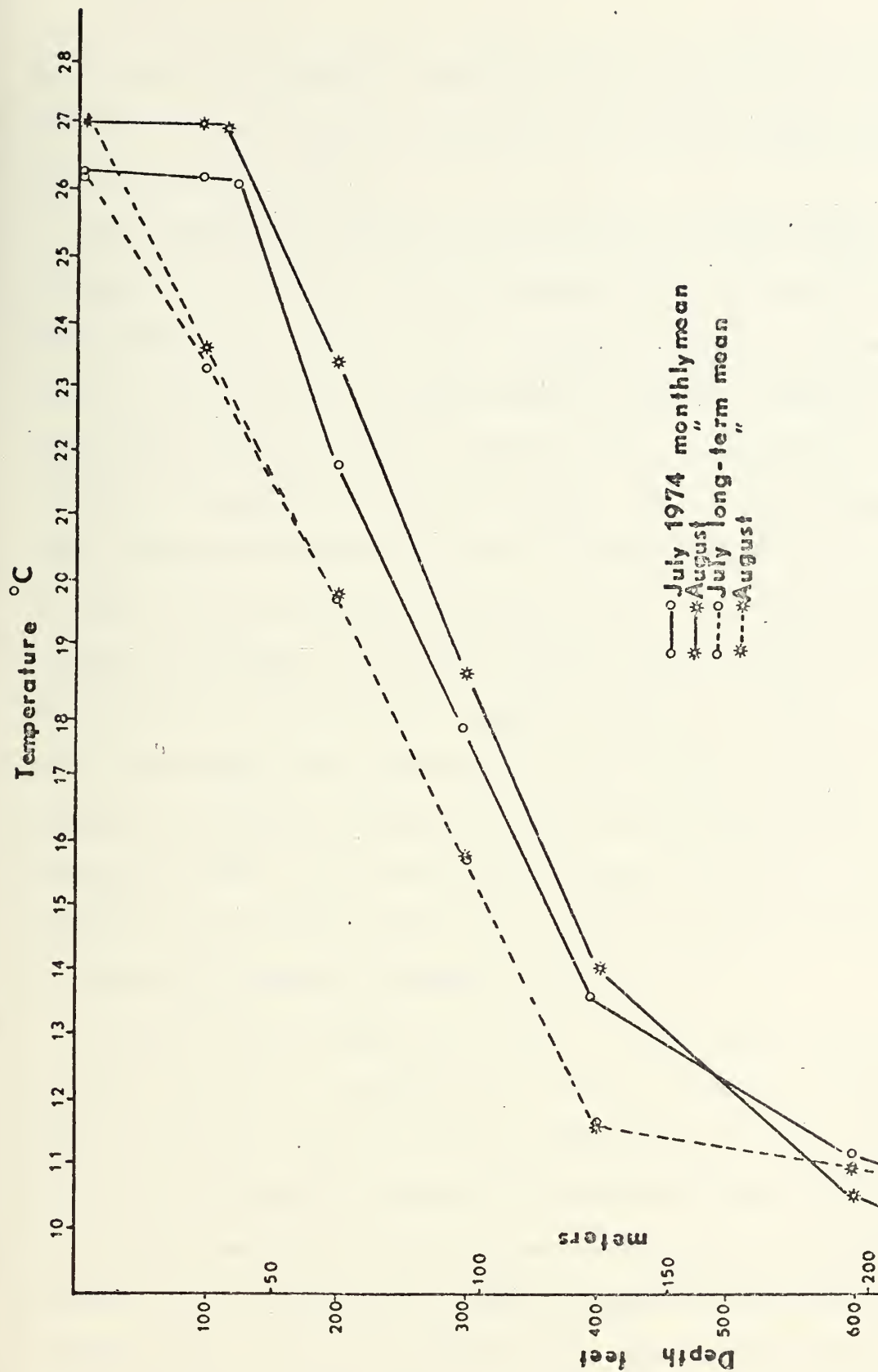


Figure 18. 1974 Monthly Mean and Long-Term Mean Temperature Profiles for July and August near 15N, 140W.



were taken from a gridpoint located in the area of  $30 \text{ kcal cm}^{-2} \text{ mo}^{-1}$  heat storage change of Figure 2. The amount of BT data is significantly less in this area south of 20 N.

The temperature profiles for June and July near OWS November are shown in Figure 15. At this location the change in heat storage over the 30-day period was a gain of  $14 \text{ kcal cm}^{-2}$ . As shown in Figure 9 a downward heat flux of  $5 \text{ kcal cm}^{-2} \text{ mo}^{-1}$  occurred during the period. Consistent with mixed-layer model theory in this case, the heat flux is accounted for by the  $0.8^{\circ}\text{C}$  increase of temperature in the mixed layer. The average increase of temperature through the thermocline of  $0.6^{\circ}\text{C}$  accounts for the other  $9 \text{ kcal cm}^{-2} \text{ mo}^{-1}$  increase in the heat storage from June to July. The climatological profiles indicate the presence of a constant seasonal thermocline below 125 m, whereas the monthly mean profiles show a changing thermocline structure from June to July. The change in the thermocline structure during this period could have resulted from physical processes occurring below the mixed layer to depths greater than 250 m. Since the observed warming from June to July could not have been due to surface heating processes, the changes would have to be due to a warm eddy extending throughout the depth.

In Figure 16 the temperature through the mixed layer increases in response to the  $7 \text{ kcal cm}^{-2} \text{ mo}^{-1}$  downward flux of heat. However, in this case the  $0.6^{\circ}\text{C}$  increase of temperature did not balance the heat flux. The slight decrease in the temperature through the thermocline indicates physical processes are removing heat from the water column but not enough to balance the increased downward heat flux from July to August. Despite the increased rate in downward heat flux, the rate of temperature increase in the mixed layer decreased from  $0.8^{\circ}\text{C mo}^{-1}$  to  $0.6^{\circ}\text{C mo}^{-1}$ . Thorne (1974) using a method similar to Seckel (1962), showed that advection can account for such rate changes in the mixed



layer. A cold anomaly in the mixed layer during August of 1974 is depicted in Figure 16, and also indicates that physical processes could have been responsible for balancing the downward heat flux. In summary, these two figures indicate that physical processes are, possibly, equal to or greater in importance than the heat flux in balancing the monthly change in heat storage near OWS November.

Two additional temperature profiles for June and July are compared in Figure 17. These were taken from a gridpoint shown in Figure 2 to exceed  $30 \text{ kcal cm}^{-2} \text{ mo}^{-1}$  change in heat storage. Figure 10 shows that the heat flux is upward, or negative, tending to cool the ocean. Figure 17 reflects this condition with a slight temperature decrease through the mixed layer. The significant change in the thermocline structure below the mixed layer accounts for the  $30 \text{ kcal cm}^{-2} \text{ mo}^{-1}$  loss in heat storage. In both cases the thermoclines represent very large deviations from climatic conditions shown by the long-term profiles. In Figure 18 the July and August profiles at the same point are compared, and still show large deviations from climatology. In addition, the August 1974 profile significantly deviates from both the July 1974 and long-term seasonal thermocline between 50 and 150 meters and below 200 meters. These large and irregular anomalies suggest that computational errors, rather than physical processes, were responsible for large changes in the heat storage. Such computational errors could be a result of poor or sparse data in the area concerned, coupled with the nature of the analysis schemes described in Appendix A. This possible computational error occurs in other months studied in this heat budget calculation where large changes in the heat storage appear.

A second approach taken to investigate the heat storage term was to compare FNWC data with NMFS XBT soundings made by merchant vessels between





San Francisco and Hawaii. NMFS has computed values of heat storage directly from these BT observations using a scheme described in Appendix C. All values of heat storage for a month were averaged along the route to obtain monthly mean values. These were then compared to FNWC monthly mean values of heat storage.

Figure 19 shows the great circle route between San Francisco and Hawaii. XBT soundings were made every four hours along the route, giving a distribution of about 25 soundings spaced 120 to 170 km apart. Figure 19 also shows the gridpoints of the FNWC grid adjacent to the ship route. The values of heat storage computed from FMWC data were interpolated to give values along the ship route. Figures 20 and 21 compare the values of heat content during July and November 1974. Also depicted on each graph are the heat storage values derived from FMWC long-term means. Both graphs show the FNWC derived values are consistently larger than NMFS values taken from actual data. This difference ranges from  $10 \text{ kcal cm}^{-2} \text{ mo}^{-1}$  near Hawaii to over  $50 \text{ kcal cm}^{-2} \text{ mo}^{-1}$  near San Francisco. It should be pointed out that the FNWC gridpoint closest to the west coast of the United States along the ship route is about 150 km from San Francisco. However, the graphs of Figures 20 and 21 clearly show the large difference in heat content in an area where data should be frequently available for inclusion in FNWC analyses. In addition, the values derived from FNWC long-term means are generally closer to the NMFS values than the 1974 monthly means.

A time cross-section was constructed using this unique set of data, and is shown in Figure 22. Significant anomalies occur along the route between Hawaii and San Francisco and persist for periods longer than a month. In addition, seasonal changes in heat storage for the 250 m water column appear quite small in Figure 22, suggesting a rather strong tendency for conservation



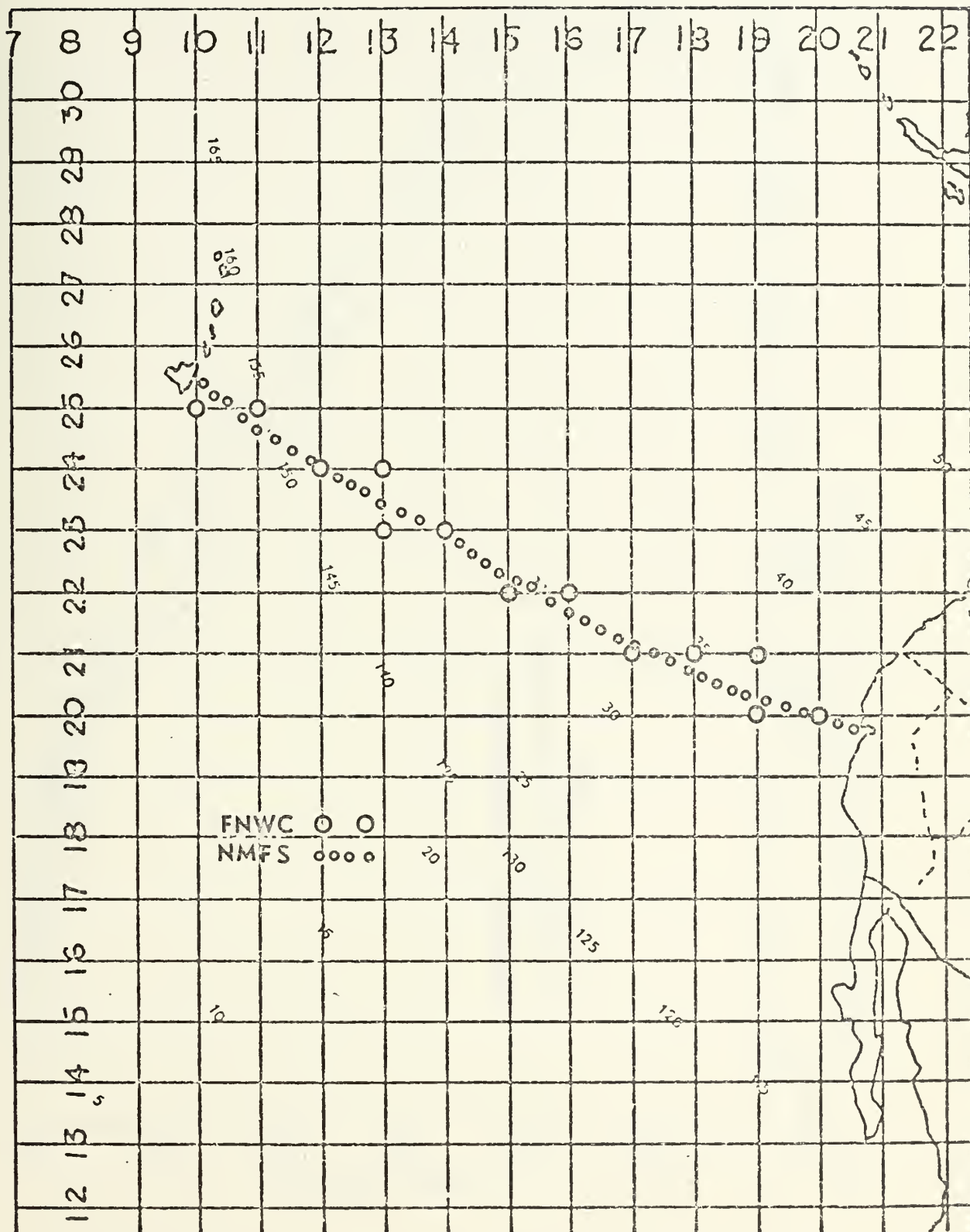


Figure 19. Great Circle Route Between Hawaii and San Francisco and FNWC Gridpoints Used in the Heat Storage Comparison.



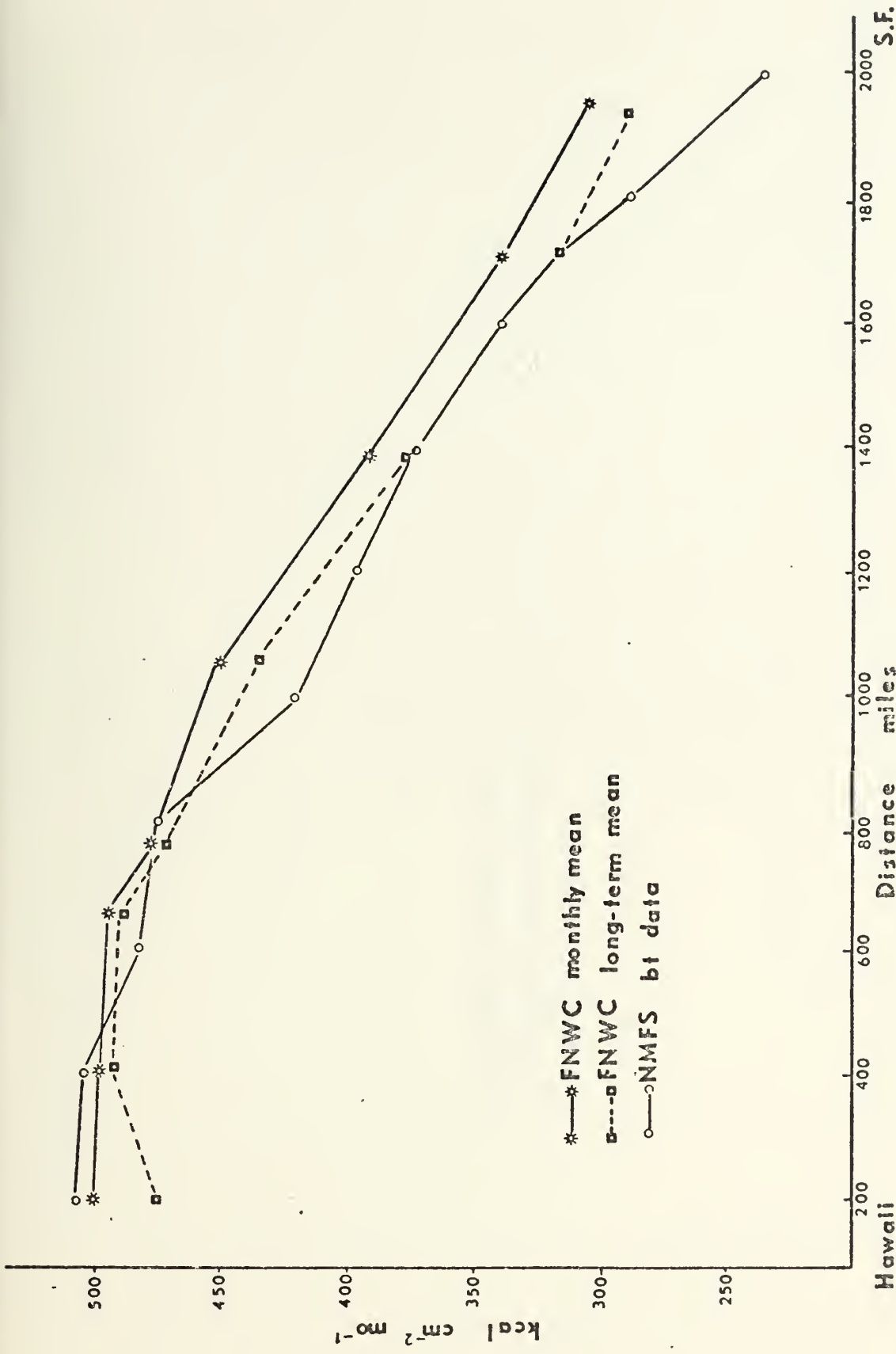


Figure 20. Comparison of NMFS Mean Heat Storage Values for June 1974 with FFWC Monthly and Long-Term Means.



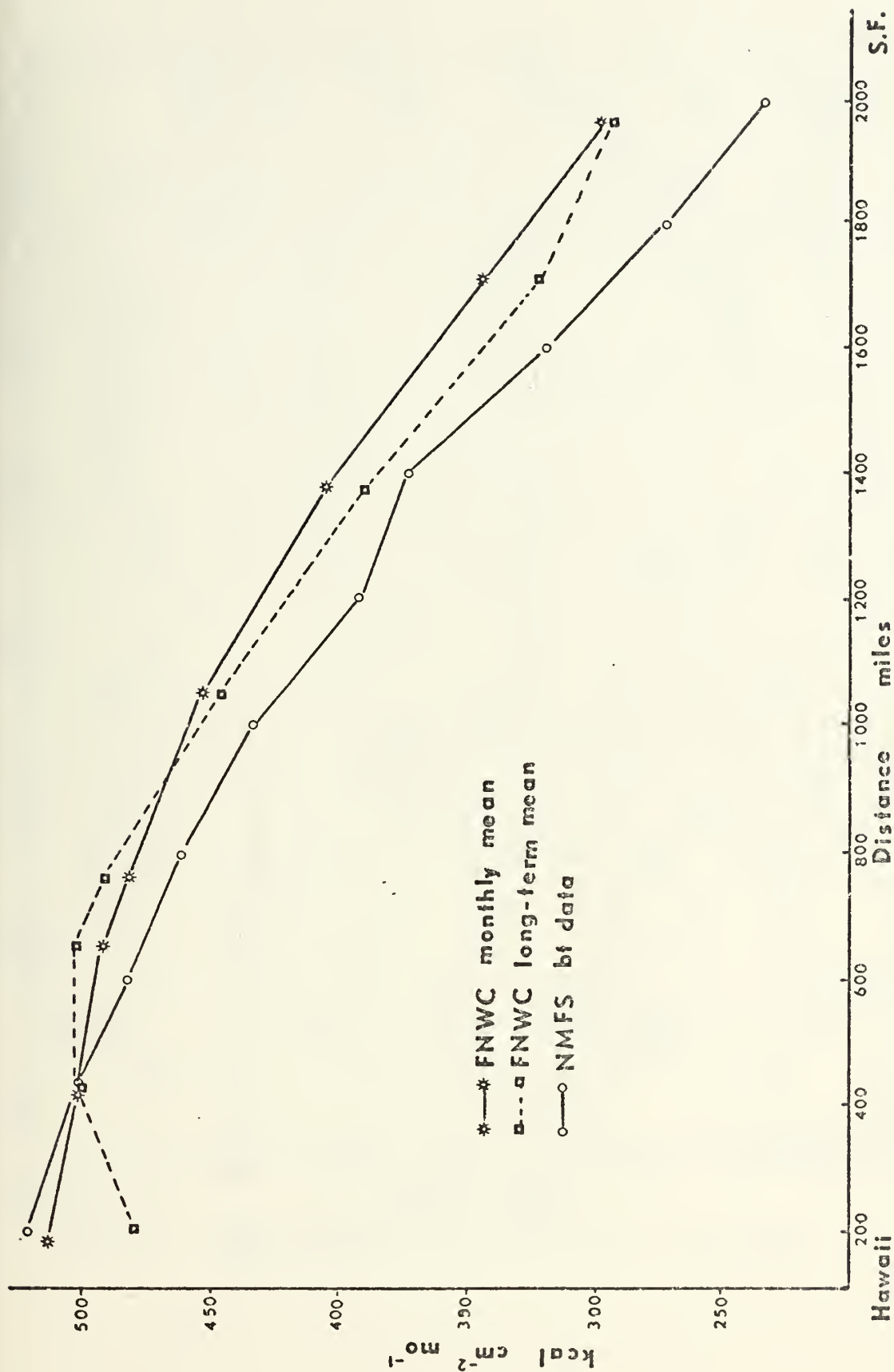


Figure 21. Comparison of NMFS Mean Heat Storage Values for November 1974 with FNWC Monthly and Long-Term Means.





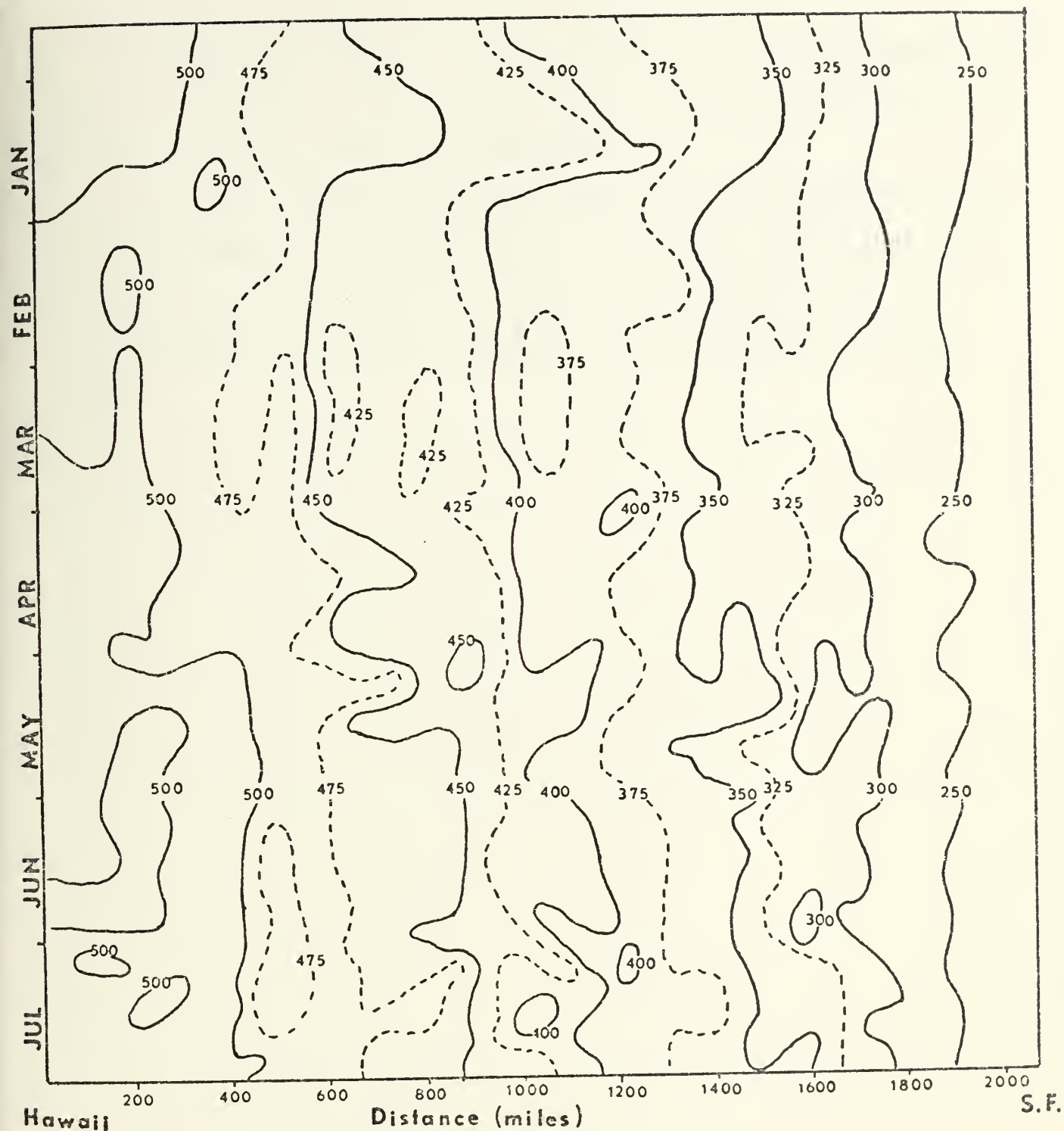


Figure 22. Time Cross-Section of NMFS Heat Storage Values ( $\text{kcal cm}^{-2}$ )



of heat in a water column of this depth. Thus, the time cross-section suggests that the large monthly changes in heat storage that occur in some areas of the eastern North Pacific are unrealistic.

In summary, it has been shown that errors in the heat storage term lead to large changes in heat storage over a 30-day period. Comparing these large changes with values of heat flux in a heat budget calculation leads to a false indication that physical processes are more important than the heat flux.



## V. SUMMARY AND CONCLUSIONS

The purpose of this study was to calculate a heat budget for the eastern North Pacific Ocean. The motivation for the study is the proposed application of mixed-layer models to ocean basin regions. Present mixed-layer models, which have been tested with point measurements, do not consider advection and diffusion. A heat budget calculation for the eastern North Pacific Ocean basin would indicate whether such models would have to be modified to include subsurface physical processes.

The primary data source for this study was the FNWC monthly mean values of sea-surface temperature, subsurface temperatures, and net heat flux which were available from September 1971 through February 1975. Data were distributed over the FNWC 63 x 63 grid, providing a space scale of 381 km at 60 N.

In this study the monthly change in heat storage for a 250 m water column was compared with the net heat flux across the sea surface. The residual, or difference between the two values, was assumed to be an indication of the physical processes involved in the balance of the heat storage change. Heat storage was computed by integrating the temperatures through the water column. The change in heat storage was compared with two separate estimates of the heat flux prepared by FNWC. The first estimate, the Total Heat Exchange ( $Q_n$ ) is based on empirical equations described in Appendix A. The second, Total Heat Flux (THF) is derived from FNWC's primitive equation model, and is described in Appendix A. In each case, large values of the residual occurred in some areas, suggesting that advection was more than three times greater than the net heat flux.

The net heat flux term was first investigated to determine possible errors in the heat budget calculation. The FNWC  $Q_n$  and THF values of net heat flux



were compared with values at OWS November derived by Dorman (1974) and over the eastern North Pacific by Clark et al. (1974). The THF values were clearly a better representation of the net heat flux than the  $Q_n$  values. However, as previously indicated, the residual values obtained in a second heat budget calculation, using THF values of heat flux were not significantly improved.

The heat storage term was also investigated as a possible source of error in the heat budget. First, in the regions of large residuals the monthly mean temperature profiles for adjacent months were compared with the long-term mean variations. Significant changes in the thermal structure well below the mixed layer depth from one month to the next indicated computational errors in analysis rather than change due to physical processes. In addition significant deviation of the monthly mean values of temperature from the long term mean in areas of sparse data coverage suggest deficiencies in analysis schemes described in Appendix A. Second, the FNWC heat storage values were compared to NMFS values of heat storage along a ship route between Hawaii and San Francisco. Consistent deviation of FNWC values also points out the problems and limitations in horizontal objective analysis schemes described in Appendix B. Finally, a time cross-section of the NMFS heat storage values was constructed. This showed that anomalous values of heat storage persist for periods longer than one month, and further indicates that the large heat storage changes derived from FNWC monthly mean data may be unrealistic.

An accurate determination of the importance of subsurface processes is difficult as a result of the discrepancies discovered in this heat budget study. However, an indication of the order of magnitude of advection and diffusion in an ocean basin is given in Figure 23. Over the portion of the eastern North Pacific Ocean studied, the median value of the residual term





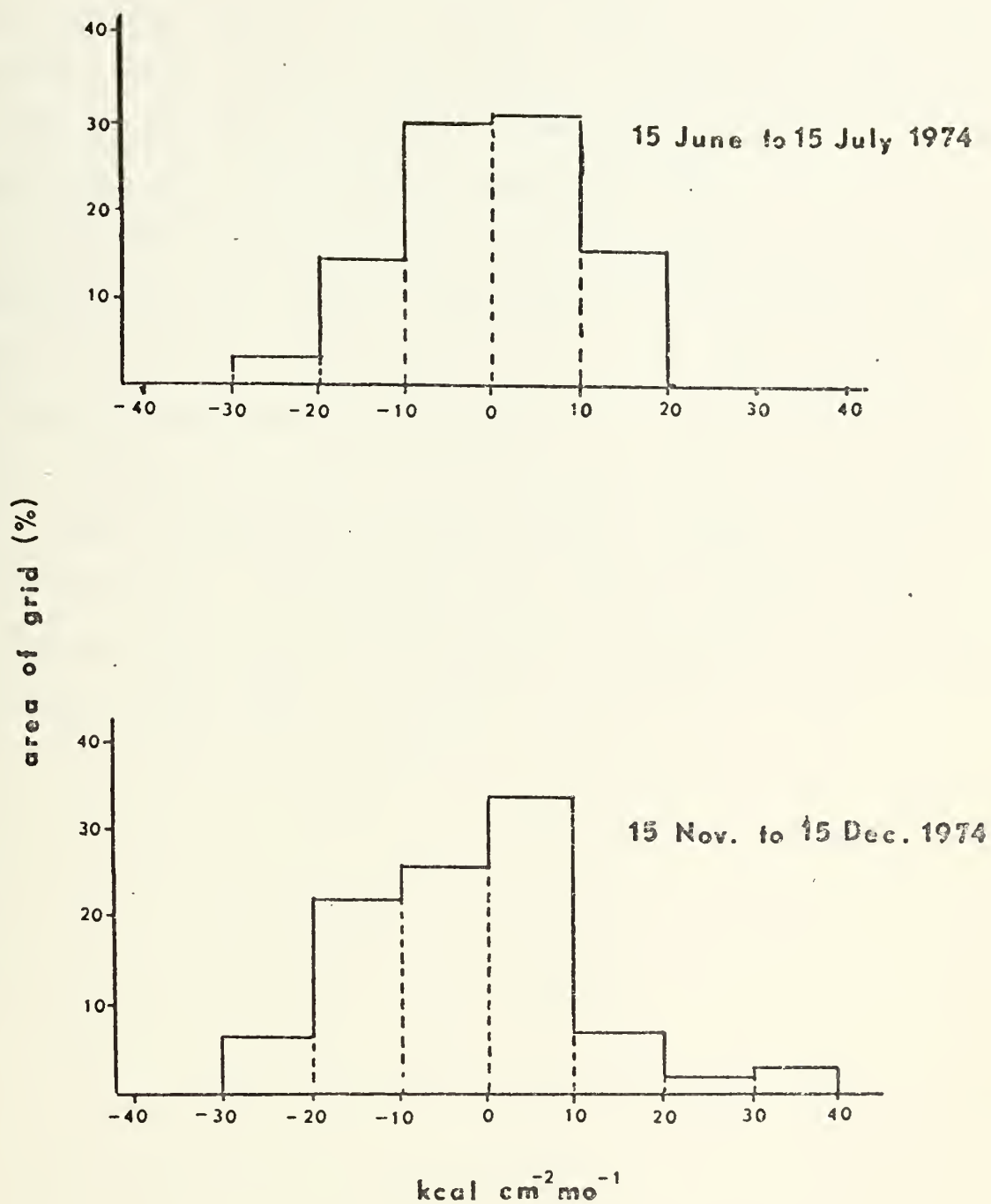


Figure 23. Percentage of FNNC Grid Covered by Significant Values of the Computed Residual



is near zero in both seasons. A negative bias was expected if advection dominated in this region, because the heat transport by the currents tends to decrease the heat storage in this region. The graphs also indicate that the magnitude of advection is about the same as the net heat flux, if the scatter shown can be attributed to computational error.

The results of this heat budget calculation suggest that Bathen (1971) overestimated the size of physical processes in the North Pacific Ocean. At the same time they do not agree with Gill and Niiler (1973) who suggested that advection and diffusion play no part in the balance of heat storage change. Computational errors in the heat storage term could be reduced by FNWC in areas of sparse data coverage, if present analysis schemes were modified to rely more on the long-term mean. Finally, mixed-layer models must take advection into account if they are to be applied on the time and space scales used in this study.



## APPENDIX A

### FNWC COMPUTERIZED PRODUCTS

The monthly mean data fields used in this study were derived from the FNWC analysis fields described below. The 00 GMT and 12 GMT analyses from each day of the month were summed and averaged to obtain the monthly mean values.

#### A. FNWC SEA SURFACE TEMPERATURE ANALYSIS

The sea surface temperature analysis is accomplished through a scheme called Fields by Information Blending (FIB). (See Appendix B.) The analysis is done on a 125 x 125 grid with an output on a 63 x 63 grid.

Inputs to the analysis are sea-surface temperature reports within six hours of the analysis time, and surface temperatures received during the past 24 hours. The first step in the analysis is to adjust the 12 hour old sea-surface temperature toward the interpolated climatological field of the analysis time. This interpolated field is a linear interpolation over two months; the present and preceding month if the day is less than 15, or the present and following month if the day is greater than 15. If the analysis is for the 15th only the climatology for the present month is used. This adjusted climatological field is then assigned a weight based on the gradient of the temperature between gridpoints; highest gradients are given the lowest weights. Next the first guess field produced by blending the previous analysis and the weighted climatology. The next step is to read and screen the sea-surface temperature reports. A difference field is computed by subtracting the first guess field from the field produced from reports. Each report is assigned a weight based on its age. The final sea-surface temperature



analysis is produced by blending this difference field with the guess fields using assigned weights.

#### B. FNWC POTENTIAL MIXED LAYER DEPTH ANALYSIS

The mixed layer depth (MLD) is defined as the lower boundary of the turbulent, mixed surface layer or the upper boundary of the thermocline. The potential mixed layer depth (POTMLD) is defined as the depth to which the turbulent mixed surface layer extends.

The initial step in the analysis is to adjust the 12-hour-old potential mixed-layer depth toward the interpolated climatological field of the analysis time. This interpolated field is a linear interpolation over two months; the present and preceding month if the day is less than 15, or the present and following month if the day is more than 15. If the analysis is for the 15th day only the climatology of the present month is used. This adjusted 12-hour-old field is the first guess field.

Next the mixed-layer depth possible due to wave mixing alone is computed from the combined wave height analysis from the following empirical formula:

$$\begin{aligned} \text{MLD}_{\text{waves}} &= \text{CH} \left[ 11. - 0.1(\text{SST} - T_{600}) \right] && \text{if } \text{SST} \geq T_{600} \\ &= \text{CH} \cdot 11. && \text{if } \text{SST} < T_{600} \end{aligned}$$

where CH = combined wave height  
SST = sea surface temperature  
T<sub>600</sub> = temperature at 600 feet

The effect of the term,  $0.1(\text{SST} - T_{600})$ , is to reduce the depth of mixing when a strong temperature gradient exists near the surface. The mixed-layer depth field due to wave action is then smoothed with a special smoothing function designed to decrease the highest values in the field without increasing the values at any point.

Next, the MLD field due to wave mixing is compared to the initial guess field produced from climatology and the deeper of the two is chosen as the





second guess MLD field. The final step in the analysis is to adjust this second guess field to BT reports taken within the past 72 hours. The reports are weighted, based on the age of the observations at analysis time, with the latest reports receiving the greatest weight. One final control placed on the analysis field is to force the layer depth to be less than or equal to 900 feet at all grid points.

This analysis scheme is subject to errors in the wave height analysis, and the empirical equation relating the MLD to the wave heights. For example  $MLD_{waves}$  does not depend on whether the waves are breaking or not.

### C. FNWC SUBSURFACE THERMAL STRUCTURE ANALYSIS

The subsurface temperature analysis is made at the following standard levels: surface, 100 feet, 200 feet, 300 feet, 400 feet, 600 feet, 800 feet, and 1200 feet. The inputs to the analysis are the 12-hour-old temperature analysis at standard levels, climatology at standard levels, the present sea-surface temperature analysis, the present mixed-layer depth analysis, and BT observations for the past 72 hours.

The first step in the analysis is to prepare guess fields for each standard level. This is done in two steps. First the 12-hour-old analysis is adjusted toward climatology; then this field is adjusted to the sea-surface temperature and the mixed-layer depth analyses to produce the final guess field. The second step is to prepare data lists from reported observations. Each report is assigned a weight factor on the basis of age, and then interpolated to find temperatures at all standard levels from the surface to the bottom of the report.

The final step is to adjust the fields to the data. First the final guess field is adjusted to the data and a light smoothing function is applied to



the vertical gradient between the level in question and the level above. This results in a first analysis field. Next, the first analysis field is adjusted to the data and a vertical control is applied requiring that the temperature at the level in question is less than or equal to the temperature of the level above. The final analysis for a level is produced after the temperature at any level is restricted to the range  $-2^{\circ}\text{C}$  to  $+35^{\circ}\text{C}$ .

The principal limitation on the accuracy of the subsurface thermal structure model is the lack of data. This means that analyses in no-data areas tend to be based mostly on climatology, only the controlling influence of the sea surface temperature analysis in the model keeps the fields quasi-synoptic.

#### D. FNWC HEAT EXCHANGE ANALYSIS

There are five components involved in a computation of heat exchange: heat absorbed from the sun, heat reflected from the sun's short wave radiation, radiated heat, sensible heat exchanged at the interface by turbulent processes, and latent heat from evaporation. Each component is calculated by a separate equation, and the results are combined to obtain the net or total heat exchange. The following equations are used in the computation of each component:

##### 1. Heat Added by Solar Insolation

$$Q_s = 0.014 A_n t_d (1.0 - 0.0006 C^3)$$

where  $Q_s$  = 24 hour insolation for clear skies

$A_n$  = noon altitude of the sun

$t_d$  = length of day

$C$  = total cloud cover in tenths

##### 2. Albedo or Reflected Solar Insolation

$$Q_r = 0.15 (Q_s) - (0.01 Q_s)^2$$

##### 3. Effective Back Radiation

$$Q_b = \sigma T_a^4 \left\{ 0.261 \exp \left[ -7.77 \times 10^{-4} (273 - T_a)^2 \right] + 4 \left( \frac{T_w - T_a}{T_a} \right) \right\} 1.0 - .0765 C$$



where  $T_a$  = air temperature  
 $T_w$  = water temperature  
 $\sigma = 4.88 \times 10^{-9} \text{ ly hr}^{-1} \text{ }^{-4}$

#### 4. Latent Heat Transfer

$$Q_e = (0.26 + 0.077 V) (0.98 e_w - e_a) L_t \quad [e_w - e_a \text{ positive}]$$

$$= 0.077 V (0.98 e_w - e_a) L_t \quad [e_w - e_a \text{ negative}]$$

where  $V$  = wind speed  $\text{m sec}^{-1}$   
 $e_w$  = saturation vapor pressure of sea surface mb  
 $e_a$  = water vapor pressure of the air mb  
 $L_t$  = latent heat of vaporization gm cal

#### 5. Sensible Heat Transfer

$$Q_h = 39 (0.26 + 0.077 V) (T_w - T_a) \quad [T_w - T_a \text{ positive}]$$

$$= 3 V (T_w - T_a) \quad [T_w - T_a \text{ negative}]$$

These five parameters are then combined to give a total heat exchange ( $Q_n$ ) as follows:

$$Q_n = Q_s - Q_r - Q_b - Q_e - Q_h$$

These empirical formulas were selected through a comprehensive literature review, and were those which promised the greatest reliability because of performance in studies supported by field testing. The accuracy of these formulas in synoptic use can be directly determined only in rare instances when a research vessel is available to make radiation measurements. Indirect verification can be done by matching net heat flux analyses against measured changes which occur in the oceans and atmosphere, as attempted in this thesis.

The errors which do occur in the heat exchange computations are probably caused by inaccuracies in the input analyses. In general, these input parameters are reasonably accurate, but errors in meteorological observations, and in the manipulating and averaging of sparse data over large sea areas, can cause problems. Cloud analyses have been one of the greatest error sources. The wind field analyses are generally good, but a small error at high wind speeds will cause large errors in some heat exchange components, particularly latent heat exchange.



## E. FNWC TOTAL HEAT FLUX ANALYSIS

The total heat flux (THF) is computed as a part of the atmospheric primitive-equation model developed for operational use at FNWC as described by Kesel and Winninghoff (1972). THF has been stored as a separate analysis since June 1974. It represents an advancement beyond the empirical formulas currently used to compute the net heat exchange at the surface. A significant difference between the primitive-equation model computation of THF and the Heat Exchange ( $Q_n$ ) model is in the calculation of heat added by solar insolation. The PE model considers net fluxes that will penetrate clouds as well as the albedo for multiple short wave scattering. Separate computations are also made for solar radiation reaching the ground for a clear sky and a cloudy sky and then combined linearly. The second component is the net long wave or effective back radiation which is also computed for both a clear and a cloudy sky. The third component, Sensible and Evaporative Heat Flux (SEHF), is computed for an ice-free ocean and for an ice-covered ocean or land depending on the area of the grid. Finally, the three components are combined to produce the total heat flux:

$$THF = SEHF - S - LWFLX$$

where  $S$  = heat added by solar radiation  
LWFLX = net long wave flux.





## APPENDIX B

### FNWC OBJECTIVE ANALYSIS

Basic to many numerical analyses is an objective analysis scheme used at FNWC. It is designed to analyze exactly to isolated observations and to a weighted mean of the observations in regions of dense data coverage. In sparse data areas, the influence of an observation is extended to a greater distance than in regions of high data density.

Prior to constructing the analysis, a gross-error check is performed on all reported data. The procedure consists of comparing each report to the interpolated value at its location in the guess field, or first approximation for the analysis. If the difference between the reported data and the guess field value exceeds a prescribed tolerance, the report is rejected.

For each reported observation which passes the gross-error check, the analysis interpolates in the guess field to the location of the observation and obtains the guess value at that point. The difference between the guess value and the reported value is computed. This difference is weighted by the distance of the observation from the four surrounding grid points. The weighted difference is then applied as a correction to the guess value at each grid point within one mesh length of the observation. Where more than one observation influences a particular grid point, the weighted mean of the corrections computed for that grid point is applied. After all guess values influenced by observed data have been corrected, the adjusted field is combined with the original guess field by a relaxation process which holds the corrected values constant. This spreads the influence of the isolated



observations while at the same time exactly fits each observation that is consistent with surrounding reports.

The Fields by Information Blending (FIB) is a new analysis technique used at FNWC for Sea Surface Temperature and Sea Level Pressure analyses. The FIB technique analyzes the distribution of a variable by blending measurements of the variable and its gradients, which come from different sources and locations.



## APPENDIX C

### NMFS COMPUTATIONAL PROCEDURES

#### A. NMFS HEAT EXCHANGE TECHNIQUE

Clark et al. (1974) prepared summaries of large scale heat exchange between the ocean and atmosphere in the eastern North Pacific Ocean for the period 1961 through 1971. The summaries were based on computations made from synoptic marine radio weather reports.

The equation for computing the energy exchange at the air-sea interface is given by:

$$Q_t = Q_{io} - Q_r + Q_b + Q_e + Q_s$$

$Q_{io}$ , the incoming solar radiation corrected for cloud cover was determined by:

$$Q_{io} = (\text{Berliand table})(1 - a C - b C^2)$$

where  $C$  = cloudiness in tenths

$b = 0.38$

$a$  = a function of latitude

Berliand's table lists the values of incoming solar radiation with a clear sky by months and latitude. The values of "a" were given by Johnson et al. (1965).

The amount of incoming solar radiation reflected at the sea surface is computed by:

$$Q_r = Q_{io} \cdot r$$

where  $r$  = percentage of radiation reflected given in a table by Budyko (1956).

The effective back radiation was computed from the equation:

$$Q_b = - \left[ s \sigma (\theta_s)^4 (0.39 - 0.050 \sqrt{e_a}) (1 - kC^2) + 4 s \sigma \theta_s^3 (\theta_s - \theta_a) \right]$$



where  $s = 0.97$  (the ratio of the radiation of the sea surface to a black body)

$\theta_s$  = absolute sea surface temperature ( $^{\circ}\text{K}$ )

$\theta_a$  = absolute air temperature ( $^{\circ}\text{K}$ )

$\sigma = 1.175 \times 10^{-7}$  (the Stefan-Boltzman constant)

$e_a$  = vapor pressure (mb)

$K$  = a function of latitude, values given in Johnson et al. (1965)

$C$  = cloudiness in tenths of a celestial dome covered

The latent heat transfer by evaporation was computed using:

$$Q_e = -4.70 (e_s - e_a) W$$

where  $e_s$  = saturation vapor pressure at temperature of sea surface (mb)

$e_a$  = vapor pressure of air (mb)

$W$  = wind speed ( $\text{m sec}^{-1}$ ).

Sensible heat transfer is given by:

$$Q_s = -3 (T_s - T_a) W$$

where  $T_s$  = sea temperature ( $^{\circ}\text{C}$ )

$T_a$  = air temperature ( $^{\circ}\text{C}$ )

$W$  = wind speed ( $\text{m sec}^{-1}$ ).

#### B. NMFS METHOD FOR COMPUTING HEAT STORAGE FROM XBT DATA

The temperature profile recordings obtained from the merchant vessel XBT measurements are sent to NMFS for processing. Each trace is digitized at inflection points in the profile. Temperatures are analyzed to hundredths of  $^{\circ}\text{C}$  with inflection points spaced approximately 10m apart.

To calculate the total heat storage for a given temperature profile an interpolation scheme is used to produce values for the following layers: 0-50 m, 0-100 m, 0-150 m, 0-200 m, 0-250 m, 0-300 m, 0-400 m, and 0-500 m. The first step in the interpolation scheme is to average the sea-surface temperature and the temperature at the first inflection point beneath the sea surface. This averaged temperature is then multiplied by the specific heat and density of sea water and the depth of the water column from the surface to the first inflection point. Next, the second inflection point is averaged with the first and multiplied by the thickness of the layer between





the two points, and the specific heat and density of sea water. The final step is to add the two values of heat storage. The process continues with each succeeding pair of inflection points derived from the original profile.

This interpolation scheme, using temperature values analyzed to a hundredth of a degree Celsius approximately every 10 m, should give highly accurate values of the actual total heat storage. On the other hand, the interpolation scheme used with the FNWC thermal data in this study could only incorporate the sea surface temperature and six subsurface temperatures to approximate the total heat storage of the 250 m water column.



## BIBLIOGRAPHY

- Bathen, K. H., "Heat Storage and Advection in the North Pacific Ocean," Journal of Geophysical Research, V. 76: 676-687, 1971.
- Bowden, K. F., M. R. Howe, and R. L. Tait, "A Study of the Heat Budget Over a Seven-Day Period at an Ocean Station," Deep-Sea Research, V.17: 401-411, 1970.
- Budyko, M. I., "Teplovoy Balans Zemnoy Poverkhnosti (The Heat Balance of the Earth's Surface)," (In Russian) Gidrometeorol. Izd, 255 pp., 1956.
- Clark, N. E., L. Eber, R. M. Laurs, J. A. Renner, and J. T. F. Saur, "Heat Exchange Between Ocean and Atmosphere in the Eastern North Pacific for 1961-71," NOAA Technical Report NMFS SSRF-682, 108pp., 1974.
- Dorman, C. E., Analysis of Meteorological and Oceanographic Data from Ocean Station Vessel N (30N, 140W), Ph. D. Thesis, Oregon State University, Corvallis, 136pp., 1974.
- Gill, A. E., and P. P. Niiler, "The Theory of the Seasonal Variability in the Ocean," Deep-Sea Research, V. 20: 141-177, 1973.
- Johnson, J. H., G. A. Flittner, and M. W. Cline, "Automatic Data Processing Program for Marine Synoptic Radio Weather Reports," U. S. Fish and Wildlife Service, SSRF-503, 74pp., 1965.
- Kesel, P. G., and F. J. Winninghoff, "The Fleet Numerical Weather Central Operational Primitive Equation Model," Monthly Weather Review, V. 100, 360-373, 1972.
- Kraus, E. B., and J. S. Turner, "A One Dimensional Model of the Seasonal Thermocline, II. The General Theory and Its Consequences," Tellus, V. 19: 98-106, 1967.
- Seckel, G. H., "Atlas of the Oceanographic Climate of the Hawaiian Islands Region," Fisheries Bulletin of Fish and Wildlife Service, U. S., V. 61: 371-427, 1962.
- Thorne, L. M., The Effects of Heat Exchange and Thermal Advection on the Rate of Change of Temperature at Ocean Weather Station November, Master's Thesis, U. S. Naval Postgraduate School, Monterey, 93pp., 1974.
- Wyrski, K., and K. Haberland, "On the Redistribution of Heat in the North Pacific Ocean," Journal of the Oceanographical Society of Japan, V. 24, No. 5; 220-233, 1968.



# INITIAL DISTRIBUTION LIST

	No. copies
1. Defense Documentation Center Cameron Station Alexandria, Virginia 22314	2
2. Library, Code 0212 Naval Postgraduate School Monterey, California 93940	2
3. Naval Oceanographic Office, Code 5221 Washington, D.C. 20373	8
4. Professor R. L. Elsberry, Code 51Es Department of Meteorology Naval Postgraduate School Monterey, California 93940	10
5. Professor G. J. Haltiner, Code 51 Department of Meteorology Naval Postgraduate School Monterey, California 93940	1
6. Department of Oceanography, Code 58 Naval Postgraduate School Monterey, California 93940	1
7. Ensign R. T. Schnoor, USN 138 Hamiltonian Drive Red Bank, New Jersey 07701	2
8. Commanding Officer Fleet Numerical Weather Central Naval Postgraduate School Monterey, California 93940	1
9. Commanding Officer Environmental Prediction Research Facility Naval Postgraduate School Monterey, California 93940	1
10. Pacific Environmental Group National Marine Fisheries Service Naval Postgraduate School Monterey, California 93940	2













22 FEB 77  
9 MAR 78

23888  
24484

Thesis

161013

S33797 Schnoor  
c.1

Monthly heat budget  
calculations for the  
eastern North Pacific  
Ocean using synoptic-  
scale data.

22 FEB 77  
9 MAR 78

23888  
24484

161013

Thesis

S33797 Schnoor

c.1

Monthly heat budget  
calculations for the  
eastern North Pacific  
Ocean using synoptic-  
scale data.

thesS33797

Monthly heat budget calculations for the



3 2768 002 00393 1

DUDLEY KNOX LIBRARY